

Asymmetric Membrane Tablet Coatings
For
Controlled–Release of Drugs

By
Hacer YENAL

A Dissertation Submitted to the
Graduate School in Partial Fulfillment of the
Requirements for the Degree of

MASTER OF SCIENCE

Department: Chemical Engineering
Major: Chemical Engineering

İzmir Institute of Technology
İzmir, Turkey

We approve the thesis of **Hacer YENAL**

Date of Signature

.....

27.09.2002

Assoc. Prof. Dr. Sacide ALSOY ALTINKAYA

Supervisor

Department of Chemical Engineering

.....

27.09.2002

Assist. Prof. Dr. Sedat AKKURT

Co-Supervisor

Department of Mechanical Engineering

.....

27.09.2002

Prof. Dr. Semra ÜLKÜ

Department of Chemical Engineering

.....

27.09.2002

Prof. Dr. Devrim BALKÖSE

Department of Chemical Engineering

.....

27.09.2002

Assist. Prof. Dr. Oğuz BAYRAKTAR

Department of Chemical Engineering

.....

27.09.2002

Prof. Dr. Devrim BALKÖSE

Head of Department

ACKNOWLEDGEMENTS

I would like to express my sincere gratitude to Associated Professor Sacide Alsoy Altinkaya for her supervision, support, guidance and encouragement during this study and in the preparation of this thesis.

I also would like to thank to Assistant Professor Sedat Akkurt for his guidance, help and recommendations.

I am very grateful to Assistant Professor Yeşim Karasulu from Ege University, Faculty of Pharmacy, for her help and valuable suggestions.

I also wish to thank to Associated Professor Ahmet Yemeniciođlu for his comments and help for construction of experimental-set up.

Special thanks to Bülent Özbaş for his help and friendship.

I also present my deepest thanks to Deniz Şimşek because of not only his friendship but also his kind efforts, helps and endless support.

I would like to appreciate deeply to my friends: Şule Uçar, Berna Topuz, Sevdıye Atakul, Mehmet Gönen and Gökhan Erdoğan for their friendships and encouragements.

I would like to express my thanks to Murat Pakel for his help, support and understanding during this study.

Finally, I could not be able to complete this thesis without encouragements and understandings of my family.

ABSTRACT

Most of the controlled release systems developed for drug delivery applications depend on membrane technology. The dense structure of the membrane in conventional controlled release systems prolongs the release of drug. To eliminate this disadvantage while maintaining the benefits of dense membrane systems, an asymmetric type of coating was applied on tablets. Coatings were prepared from cellulose acetate, acetone, water solution by phase inversion technique. To determine the release rate of drug, dissolution studies on tablets were performed according to United States of Pharmacopeia (USP). In these studies, the effects of composition of the polymer/solvent/nonsolvent, coating time, number of coating layers, evaporation conditions and the nonsolvent type on the release rate of the drug and the structure of membrane were investigated. Experiments were designed using commercial software package Design-Expert and a quadratic model equation was obtained to predict the effect of composition of cellulose acetate, acetone and water on the release rate of drug. The advantage of asymmetric type coating over the conventional dense type coating was further demonstrated by measuring the permeabilities of both type of coatings. In addition, the structures of membranes were analyzed using scanning electron microscope (SEM) micrographs.

ÖZ

İlacın vücutta kontrollü salımı için geliştirilen sistemlerin birçoğu membran teknolojisine dayalıdır. Geleneksel kontrollü salım sistemlerinde kullanılan yoğun yapıdaki membranlar ilaç salımını uzatmaktadır. Bu dezavantajı ortadan kaldırmak için, yoğun yapıdaki membran sistemlerinin yararları sabit tutularak tabletlere asimetric yapıdaki kaplamalar uygulanmıştır. Kaplamalar faz ayırımı yöntemi ile selüloz asetat, aseton ve su çözeltisi kullanılarak hazırlanmıştır. İlacın salım hızını belirlemek için, tabletlerin çözünme çalışmaları United States Pharmacopeia (USP) standartlarına göre yapılmıştır. Bu çalışmalarda, polimer/çözücü/çözücü olmayan kompozisyonlarının etkileri, kaplama zamanı, kaplama sayısı, buharlaşma koşulları ve çözücü olmayan malzemenin ilaç salım oranına ve membran yapısına etkisi incelenmiştir. Deneyler ticari bilgisayar yazılım programı Design-Expert kullanılarak tasarlanmış ve selüloz asetat, aseton ve su kompozisyonunun ilaç salımına etkisini belirlemek için kuadratik model denklemi elde edilmiştir. Asimetric yapıdaki kaplamaların geleneksel yoğun yapıdaki membrana göre avantajı, her iki tipteki kaplamaların geçirgenlikleri ölçülerek de kanıtlanmıştır. Buna ek olarak, taramalı elektron mikroskobu fotoğrafları incelenerek membran yapıları analiz edilmiştir.

TABLE OF CONTENTS

LIST OF FIGURES.....	iv
LIST OF TABLES	viii
CHAPTER 1. INTRODUCTION	1
CHAPTER 2. CONTROLLED-RELEASE SYSTEMS.....	3
2.1. Advantages and Disadvantages of Controlled-Release Systems	4
2.2. Classification of Controlled-Release Systems	5
2.2.1. Diffusion-Controlled Release Systems.....	5
2.2.1.1. Reservoir Systems	5
2.2.1.2. Matrix Systems	8
2.2.2. Chemically-Controlled Systems	8
2.2.2.1. Bioerodible Systems	8
2.2.2.2. Pendant Chain Systems	9
2.2.3. Swelling – Controlled Systems	10
2.2.4. Magnetically - Controlled Systems	11
2.3. Polymers For Drug Release Formulations	11
2.4. Release Kinetics	12
CHAPTER 3. PREVIOUS STUDIES ON CONTROLLED-RELEASE SYSTEMS	14
3.1. Matrix Systems.....	14
3.2. Bioerodible Systems.....	16
3.3. Swelling Systems	16
3.4. Membrane Systems	17

CHAPTER 4. DIFFUSION IN ASYMMETRIC MEMBRANES.....	20
4.1. Diffusion in Dense Membranes.....	20
4.2. Diffusion in Asymmetric Membranes.....	20
4.3. Diaphragm Cell Model.....	22
CHAPTER 5. STATISTICAL DESIGN AND ANALYSIS OF EXPERIMENTS	25
5.1. Experimental Designs for Fitting Response Surfaces	25
5.2. Mixture Design.....	27
5.3. Mixture Models.....	28
CHAPTER 6. EXPERIMENTAL.....	30
6.1. Properties of Polymer and Model Drug	30
6.2. Tablet Preparation	32
6.3. Tablet Coating.....	32
6.3.1. Preparation of Membrane Solution	32
6.3.2. Dip-Coating.....	33
6.4. Dissolution Studies.....	33
6.5. Permeability Studies.....	35
6.6. Characterization	36
CHAPTER 7. RESULTS AND DISCUSSION.....	37
7.1. Dissolution and Morphological Studies	37
7.1.1. Comparison of the Drug Release Rates of Dense and Asymmetric Membrane Coated Tablets	40
7.1.2. Effect of Polymer / Solvent (P/S) Ratio on Release Rate.....	42
7.1.3. Effect of Polymer / Nonsolvent (P/NS) Ratio on Release Rate.....	48

7.1.4. Effect of Solvent / Nonsolvent (S/NS) Ratio on Release Rate.....	49
7.1.5. Effect of Number of Coatings on Release Rate....	51
7.1.6. Effect of Coating Time on Release Rate	52
7.1.7. Effect of Evaporation Conditions on Release Rate.	52
7.1.8. Effect of Types of Nonsolvent on Release Rate...	54
7.2. Permeability Studies.....	60
7.3. Statistical Analysis of Experiments.....	62
7.3.1. Determination of the Variables and Feasible Region for the Design of Experiments.....	62
7.3.2. Mixture Design.....	62
7.3.3. The Regression Model and Statistical Analysis ...	65
7.3.4. The Response Surface Plot.....	67
CONCLUSIONS.....	70
REFERENCES	72
APPENDIX A	
APPENDIX B	
APPENDIX C	

LIST OF FIGURES

Figure 2.1. Concentration profiles for (a) conventional (b) controlled-release formulations.	3
Figure 2.2. Idealized diffusion-controlled reservoir release system	6
Figure 2.3. Schematic diagram of the osmotic tablet system surrounded by membrane drilled with two orifices.	7
Figure 2.4. Idealized diffusion-controlled matrix tablets.....	8
Figure 2.5. Idealized drug release from bioerodible systems (a) surface erodible (b) bulk erodible.....	9
Figure 2.6. Idealized drug release from pendant chain systems.....	10
Figure 2.7. Idealized swelling-controlled release system.	10
Figure 2.8. Comparison of release kinetics from conventional (first-order) and controlled-release formulations.	13
Figure 4.1. Schematic cross section of an asymmetric membrane and the mass transport resistance configuration.	22
Figure 5.1. Simplex lattice design for a ternary mixture.	28
Figure 6.1. SEM micrograph of crystalline theophylline anhydrate.	30
Figure 6.2. Molecular structure of theophylline.....	31
Figure 6.3. Molecular structure of cellulose.	31
Figure 6.4. Dissolution test apparatus.....	34
Figure 6.5. Schematic representation of diffusion cell.	35
Figure 7.1. Release of theophylline from tablets coated with dense and asymmetric-membrane coatings.	40
Figure 7.2. SEM micrograph of cross section of a membrane. Initial composition: 10% CA, 80% Acetone, 10% Water. Magnificationx5000.	41

Figure 7.3. SEM micrograph of cross section of a membrane. Initial composition: 10% CA, 90% Acetone. Magnificationx10000.	41
Figure 7.4. Release rate of theophylline as a function of P/S ratios for 5%, 10% and 15% water content.....	43
Figure 7.5. SEM micrograph of cross section of a membrane. Initial composition: 15% CA, 80% Acetone, 5% Water. Magnificationx5000	43
Figure 7.6. SEM micrograph of cross section of a membrane. Initial composition: 10% CA, 85% Acetone, 5% Water. Magnificationx5000.	44
Figure 7.7. SEM micrograph of cross section of a membrane. Initial composition: 5% CA, 90% Acetone, 5% Water. Magnificationx10000.	44
Figure 7.8. SEM micrograph of cross section of a membrane. Initial composition: 5% CA, 85% Acetone, 10% Water. Magnificationx500.	45
Figure 7.9. SEM micrograph of cross section of a membrane. Initial composition: 15% CA, 75% Acetone, 10% Water. Magnificationx4000.	45
Figure 7.10. SEM micrograph of cross section of a membrane. Initial composition: 5% CA, 80% Acetone, 15% Water. Magnificationx10000.	46
Figure 7.11. SEM micrograph of cross section of a membrane. Initial composition: 10% CA, 75% Acetone, 15% Water. Magnificationx10000.	47
Figure 7.12. SEM micrograph of cross section of a membrane. Initial composition: 15% CA, 70% Acetone, 15% Water. Magnificationx10000.	47
Figure 7.13. Release rate of theophylline as a function of P/NS ratio for 80% acetone content.....	48
Figure 7.14. SEM micrograph of cross section of a membrane. Initial composition: 3% CA, 80% Acetone, 17% Water. Magnificationx5000.	49
Figure 7.15. Release rate of theophylline as a function of S/NS ratio for 10% and 15% polymer content.	50

Figure 7.16. Release of theophylline from tablets coated with asymmetric membrane 1, 2 and 3 times.	51
Figure 7.17. Release of theophylline from tablets coated with asymmetric membrane with coating times 1 and 2 min.	52
Figure 7.18. Release of theophylline from tablets in which the solvent is evaporated under free and forced convection condition.	53
Figure 7.19. SEM micrograph of cross section of a membrane. Initial composition: 10% CA, 80% Acetone, 10% Water under forced convection condition. Magnificationx15000.....	53
Figure 7.20. The release of theophylline from tablet coatings prepared from CA/Acetone and different nonsolvents and the skin percents of these membranes.....	55
Figure 7.21. SEM micrograph of cross section of a membrane. Initial composition: 10% CA, 80% Acetone, 10% Octanol. Magnificationx10000.	56
Figure 7.22. SEM micrograph of cross section of a membrane. Initial composition: 10% CA, 80% Acetone, 10% Octanol. Magnificationx20000.	56
Figure 7.23. SEM micrograph of cross section of a membrane. Initial composition: 10% CA, 80% Acetone, 10% Formamide. Magnificationx5000...	57
Figure 7.24. SEM micrograph of cross section of a membrane. Initial composition: 10% CA, 80% Acetone, 10% Glycerol. Magnificationx1250.	57
Figure 7.25. SEM micrograph of cross section of a membrane. Initial composition: 10% CA, 80% Acetone, 10% Hexanol. Magnificationx5000.	58
Figure 7.26. SEM micrograph of the top layer of membrane. Initial composition: 10% CA, 80% Acetone, 10% Hexanol. Magnificationx20000.	58
Figure 7.27. SEM micrograph of the mid section of membrane. Initial composition: 10% CA, 80% Acetone, 10% Hexanol. Magnificationx10000.	59

Figure 7.28. Relationship between the percentage of skin layer and $P_{\text{eff}} / P_{\text{dense}}$ ratio.....	61
Figure 7.29. The feasible region for the design of experiments.....	63
Figure 7.30. The constrained experimental region the design of experiments. .	64
Figure 7.31. Contour plots in the D-optimal design area.....	67
Figure.7.32. Three dimensional surface plot for design area.	69

LIST OF TABLES

Table 6.1. Properties of chemicals used for drug-release experiments.....	33
Table 7.1. Release rates and characterization of membranes prepared for dissolution studies.....	38
Table 7.2 Calculated resistances of skin layer, substrate, polymer and pores of the membranes.....	39
Table 7.3. The release rate and the results of phase analysis of the membranes prepared from different nonsolvents.....	55
Table 7.4. Permeability and thickness of the membranes.....	60
Table 7.5. D-optimal design for the mixture of membrane solution.	64
Table 7.6. Analysis of Variance (ANOVA) for the release rate data.....	66
Table 7.7. Statistical analysis of the release rate data.....	66

CHAPTER 1

INTRODUCTION

The use of different systems as a means of delivering a wide variety of active ingredients such as drugs, pesticides, fragrances at a specified rate and a desired location for a specified period of time is called “Controlled-Release” Technology. Studies on “controlled-release systems” began to be developed for agricultural products in the 1950’s, and such approaches were extended to medicine in the 1960’s.

The significant growth of controlled-release technology for drug delivery applications was due to general-dose delivery problems. During conventional treatments, drug concentration may exceed maximum toxic level or may fall below the ineffective level requiring to take several doses, so increasing the likelihood of unwanted side effects. To prevent these problems, different controlled-release systems were developed to deliver the optimum doses at the right time and to the right place.

Among the many controlled-release systems developed and commercialized since 1950’s, the most widely used ones depend on membrane technology. In these systems the release of drug surrounded by a swollen or non-swollen polymeric membrane is controlled by diffusion of drug through the membrane. The structure of the membrane in conventional controlled-release systems is usually dense and symmetric, thus influx of water into the membrane is slow, prolonging the release of drug. This is a principal problem with dense membrane coatings. To increase the permeability of the membrane, thus to achieve useful drug release rates, various attempts have been reported, including plasticizers and water-soluble additives incorporated in the coating and multilayer composite coatings. To increase coating permeability further, a new type of membrane coating has been developed, that offers significant advantages over the membrane coatings used in conventional tablets. These membranes consist of a thin, dense outer skin layer supported on a highly permeable, thicker and porous layer that provides mechanical strength and durability. The drug release rates from tablets or capsules coated with this new type of membranes can be adjusted by controlling the membrane structure without changing coating material or varying the coating thickness.

In this study, the last novel approach was adopted and asymmetric membrane coated drug tablets were prepared by phase inversion process. Drug tablet is coated by first dipping into the membrane forming solution and then allowing it to dry. The coating solution consists of polymer, solvent and nonsolvent, which does not dissolve the polymer completely. During evaporation, initially homogeneous polymer solution becomes unstable and is separated into polymer lean and polymer rich phases. As a result, asymmetric type of coating is obtained.

Throughout this study, cellulose acetate was chosen as a membrane-forming polymer since it is a water-insoluble, biodegradable and natural polymer, acetone was used as a solvent and theophylline was chosen as a model drug.

The dissolution studies on coated tablets were performed according to United States Pharmacopoeia (USP) standards. In these studies different nonsolvents were used in solution to investigate their effect on membrane structure. Additionally, the effects of the initial composition of the solution, number of coating layer, coating (dipping) time and the evaporation condition on the structure of the membrane and the release rate of theophylline were examined. In order to draw meaningful and objective conclusions from the data, statistical design of experiments was performed for cellulose acetate, acetone, water system using commercial software package called Design-Expert. In the design of the experiments, the release rate of theophylline was chosen as the response, while composition of cellulose acetate, acetone and water were considered as variables affecting the response. In order to further demonstrate the advantages of the asymmetric type of coatings, the permeability of different membranes prepared by varying the compositions of the polymer/solvent/nonsolvent were also measured. In addition, the morphology of the membranes was observed using scanning electron microscope.

CHAPTER 2

CONTROLLED-RELEASE SYSTEMS

Controlled-release technologies are designed to deliver active agents at a specified rate, at a desired body site for a specified period of time. The goal of the rate-controlled technology is to produce a convenient, generally self-administered dosage form that yields a constant infusion of the drug.

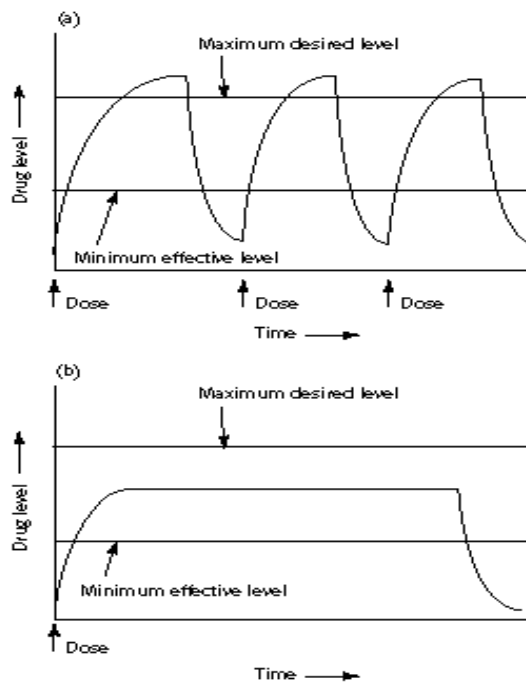


Figure 2.1. Concentration profiles for (a) conventional (b) controlled-release formulations.

Controlled-release formulations offer

- greater efficacy because optimal concentrations of active ingredient can be maintained in the environment of use
- improved safety from reliable release kinetics and control over the amount of active ingredient available at any one time

- greater convenience because fewer applications or treatments are needed

Controlled-release dosage forms provide sustained drug release and require less frequent drug loading than conventional forms. This is an important advantage for patient compliance during medication.

Patients required to take 1 or 2 dosage unit a day are thought to be less likely to forget a dose than if they were required to take their medication 3 or 4 times a day. Further, controlled-release dosage forms allow whole day coverage and help to reduce the need for the patient to be awakened for an early morning dosing. Also, depending upon the medication and the dosage form, the daily cost to the patient may be less frequent dosage administration (Ansel and Popovivch, 1990).

2.1. Advantages and Disadvantages of Controlled-Release Systems

In controlled-release systems, plasma drug levels are maintained in a therapeutically desirable range. Drug blood level fluctuations are reduced that means by controlling the rate of drug release, “peaks and valleys” of drug-blood or –serum levels are eliminated. Rate-controlled products deliver more than a single dose of medication and thus are taken less often than conventional forms (Ansel and Popovivch, 1990) so dosing frequency is reduced. Harmful side effects are minimized. Because there are seldom drug blood level peaks above the drug’s therapeutic range, and into the toxic range, adverse side effects are less frequently encountered (Ansel and Popovivch, 1990). Patient convenience and compliance are improved. With less frequency of dose administration, the patient is less suitable to neglect taking a dose. There is also greater patient convenience with daytime and nighttime medication, and control of chronic illness (Ansel and Popovivch, 1990). Although the initial cost of rate-controlled drug delivery systems is usually higher than conventional dosage forms, the average cost of treatment over an extended time period may be lower with less frequency of dosing, enhanced therapeutic benefit, and reduced side-effects, and, reduced time period of health care personnel to dispense, administer and monitor patients (Ansel and Popovivch, 1990).

Besides the advantages of controlled-release systems, there are some disadvantages in any specific clinical application. Toxicity or lack of biocompatibility of the polymer

material used is one of these problems. Biocompatibility is very important because it relates to the ability of the polymer to remain biologically inert during implantation. Another problem is production of harmful byproducts from the polymer if it is biodegradable but this problem exists in bioerodible systems. Expense of the fabrication procedure of polymer-drug formulation is another disadvantage of controlled-release systems.

2.2. Classification of Controlled-Release Systems

2.2.1. Diffusion-Controlled Release Systems

2.2.1.1. Reservoir Systems

In these systems, a core of drug is surrounded by a rate-controlling membrane, and active agent is released by diffusion through the membrane. Several types of reservoir systems are coated tablets, beads, and particles, membrane-based pouches (e.g. transdermal drug delivery systems), and microcapsules.

A critical problem, from a pharmaceutical standpoint, is the ability to achieve zero-order release rates; the principal advantage of reservoir systems is the ease with which they can be designed to achieve these kinetics (Langer and Peppas, 1981). In other words, reservoir systems typically provide a constant rate of release over a substantial portion of the duration of release. The desired rate of release can usually be achieved by properly selecting the rate-controlling membrane. If the diffusivity and the concentration gradient across the membrane remain constant, then the release rate will be constant (zero-order release). To maintain a constant concentration gradient, the activity of the active ingredient within the reservoir must remain constant and transport to and from the membrane surfaces must be rapid with respect to transport through the membrane (Smith and Herbig, 1992). In reservoir systems release rate depends on the membrane thickness, permeability and area.

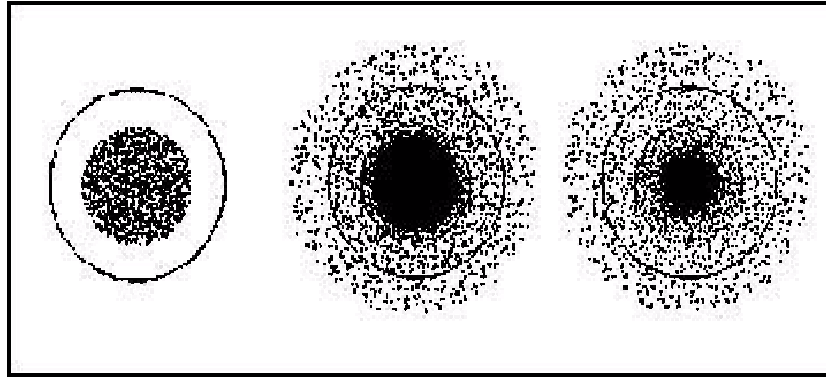


Figure 2.2. Idealized diffusion-controlled reservoir release system.

There are four types of reservoir devices:

In nonporous polymeric membranes, the active ingredient exists in a highly saturated state (with excess solid phase present) within the reservoir and is able to diffuse through the membrane in response to a gradient in thermodynamic activity. As long as the solution within the reservoir is saturated and sink conditions are maintained at the releasing film interface, the concentration gradient across the membrane remains constant and the release of the drug follows zero-order kinetics (Cahn and Haasen, 1992).

The active ingredient passes through liquid-filled pores rather than through the polymer itself in microporous membranes. To prolong release, the active agent should have a low but finite solubility in the liquid phase, which fills the pores (Cahn and Haasen, 1992).

Microencapsulation of active agents by polymeric materials is a process yielding small solid particles or liquid droplets enclosed by an intact, thin shell of polymeric material (Cahn and Haasen, 1992). The release of agent may be result of erosion of the polymeric shell or of diffusion through the shell. Commonly, release is by a combination of erosion and diffusion.

Osmotic pressure was first employed as an energy source to deliver active ingredients in the 1950s (Liu et al., 2000b). During the past some two decades, there has been a growing interest in developing osmotic pump dosage forms for controlled delivery of drugs. The elementary osmotic pump (EOP) was introduced by Theeuwes and the

coworkers in 1970s (Liu et al., 2000a). In osmotic pump systems, the core contains water-soluble drug and it is enclosed with water-permeable but drug-impermeable polymeric membrane that has a small opening. The release rate may be controlled by changing the surface area, the thickness or the nature of the membrane and by changing the diameter of the drug release orifice.

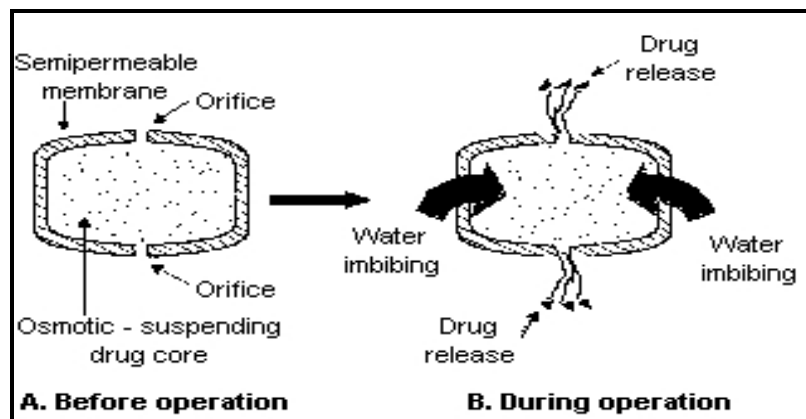


Figure 2.3. Schematic diagram of the osmotic tablet system surrounded by membrane drilled with two orifices.

Osmotic drug delivery systems are based on osmosis, the diffusion of water across a semipermeable membrane from a solution with a low osmotic pressure to a solution with a high osmotic pressure. Water is imbibed into the core through the coating; a hydrostatic pressure generated within the core forces or “pumps” a drug containing solution out of the core from delivery ports.

Osmotic systems characteristically provide a constant rate of release as long as the osmotic gradient across the rate-controlling membrane is constant and as long as the concentration of active ingredient that remains in the reservoir is constant (Smith and Herbig, 1992).

The osmotic pump tablet system for oral administration has many advantages such as (Liu et al., 2000a):

- Constant delivery rate and thereby reduced risk of adverse reactions
- Extended action period and hence improved patient compliance
- In vivo predictability of release rate on the basis of in vitro data

2.2.1.2. Matrix Systems

Matrix systems consist of active ingredients dissolved and/or dispersed throughout a polymer. If the active agent is dissolved within a nonporous polymer matrix, transport of the active agent is presumed to occur by a process involving diffusion along and between the polymer segments. If the active agent is dispersed within a polymer matrix, solute transport may occur by either a partition mechanism wherein the process involves diffusion along and between the polymer segments or a pore mechanism wherein transport occurs through microchannels that exist or are created by previous solubilization of active agent within the polymer network (Cahn and Haasen, 1992).

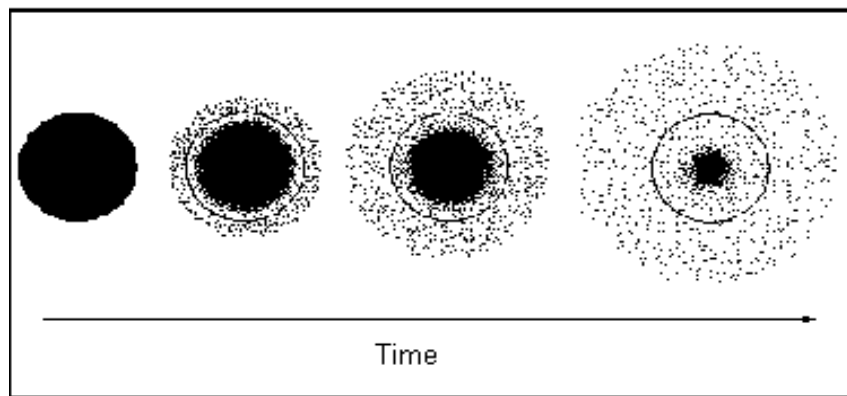


Figure 2.4. Idealized diffusion-controlled matrix tablets.

Release characteristics of matrix systems are not generally zero-order. Release rates decrease with time since the path length for diffusion increases with time as the active ingredient near the surface is released first and that in the interior must diffuse farther to be released (Smith and Herbig, 1992).

2.2.2. Chemically-Controlled Systems

2.2.2.1. Bioerodible Systems

In these systems, an active agent is dispersed into the biodegradable polymer. The release rate of the dispersed active agent may be influenced by the rate of diffusion

and/or degradation. The process of biodegradation involves systems, which must first undergo hydrolysis of covalent bonds in order to allow for concomitant solubilization of small pieces of the matrix (Cahn and Haasen, 1992). During the release process, the drug delivery in the erodible hydrophilic matrix is controlled by two mechanisms. While poorly soluble drugs are released solely by erosion of the gel, water-soluble drugs are released both by diffusion out of gelatinous layer and by the erosion of the gel (Karasulu et al., 2000).

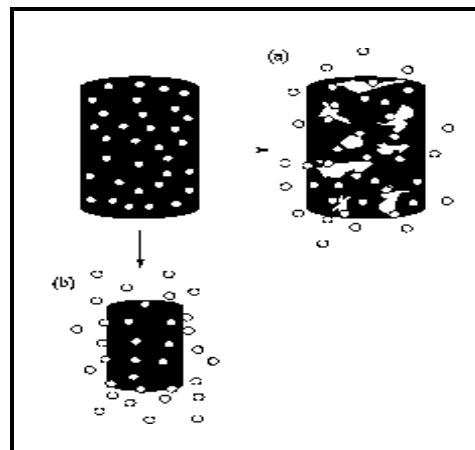


Figure 2.5. Idealized drug release from bioerodible systems (a) surface erodible (b) bulk erodible.

Bioerodible systems have a significant advantage over non-erodible systems in many applications because biodegradable polymers are eventually absorbed by the body, obviating the need for surgical removal. However, this advantage must be weighed against the potential disadvantage that the absorption products may be toxic, immunogenic, or carcinogenic (Langer and Peppas, 1981).

2.2.2.2. Pendant Chain Systems

In pendant chain systems, drug is bound to a polymer backbone chain chemically and is released by hydrolytic or enzymatic cleavage. The drug itself can be attached directly to the polymer or it can be attached via a spacer group. The spacer group may be used to affect the rate of release and hydrophilicity of the system (Langer and Peppas, 1981).

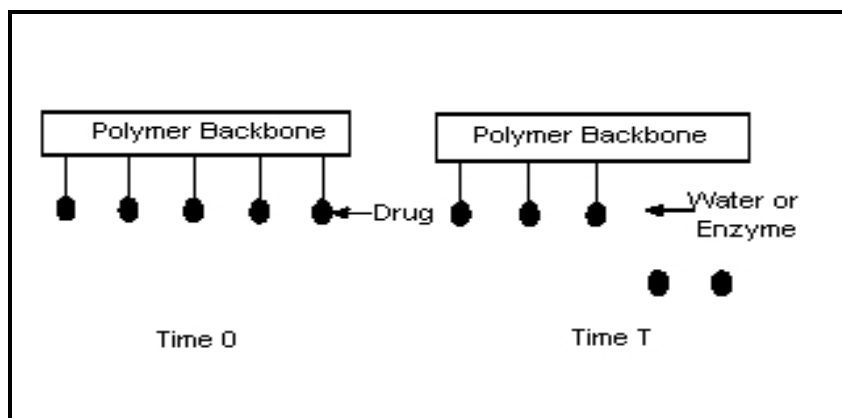


Figure 2.6. Idealized drug release from pendant chain systems.

2.2.3. Swelling – Controlled Systems

The drug is dissolved or dispersed in a polymer solution and after the evaporation of the solvent, glassy polymer matrix is obtained. Upon contact with biological fluids, water penetrates into the tablet and dissolves the drug, which then diffuses out of the tablet. In contrast to purely diffusion-controlled drug delivery systems, additionally swelling and polymer dissolution have to be taken into account. Above a certain, critical water concentration, the polymer undergoes the transition from glassy to the rubbery state, leading to dramatic changes in volume, concentration and diffusion coefficients of the involved species (Siepmann and Peppas, 2000).

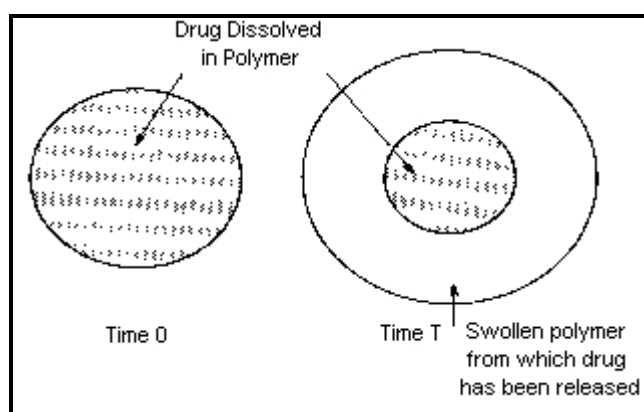


Figure 2.7. Idealized swelling-controlled release system.

In swellable matrix tablet, three fronts could be expected:

the *swelling front*, the boundary between the still glassy polymer and its rubbery state

the *diffusion front*, the boundary in the gel layer between the solid, as yet the undissolved, drug and the dissolved drug

the *erosion front*, the boundary between the matrix and the dissolution medium

The measurement of front positions provides the possibility to determine three important parameters related to the behavior of the matrix, i.e. the rate of matrix erosion, associated with the movements of the swelling front, diffusion front and erosion front, respectively (Colombo et al., 1996).

2.2.4. Magnetically - Controlled Systems

Drug and small magnetic beads are uniformly dispersed within a polymer matrix. Upon exposure to aqueous media, drug is released in a fashion typical of diffusion-controlled matrix systems. However, upon exposure to an oscillating external magnetic field, drug is released at a much higher rate (Langer and Peppas, 1981).

2.3. Polymers For Drug Release Formulations

Various types of polymers have been used in the design of drug delivery systems. The choice of the polymer and proper design of the polymer-drug formulation is of critical concern in all controlled-release formulations. The selection of polymer can

- affect diffusion and partition coefficients in diffusion-controlled systems
- affect the rate of erosion or hydrolysis in chemically-controlled systems
- affect the permeation rates of solvents in swelling-controlled systems
- presumably affect the mechanical forces in magnetically-controlled systems (Langer and Peppas, 1981)

The goal in developing a controlled-release system is to make it as close as possible to the ideal system. An ideal system should have the following characteristics. It would:

- generally display zero-order kinetics
- be inert and compatible with the environment

The toxicity, biocompatibility and immunogenicity of the polymeric device is critical because the device interfaces directly with the biological environment in which it is injected, implanted or inserted (Cahn and Haasen,1992). Therefore it should be biocompatible, non-toxic, non-mutagenic, non-carcinogenic, non-teratogenic and non-immunogenic. Additionally, it should

- be comfortable to the user
- be easily administered
- possess a high drug/polymer ratio
- be easy and inexpensive to fabricate
- be safe and free from leaks
- have good mechanical strength
- be easily sterilizable

In the case of matrix or membrane systems, one must demonstrate that the properties of the polymer are not affected by prolonged exposure to the biological environment. Furthermore, with bioresorbable systems, all polymeric degradation products as well as their metabolites must be non-toxic, non-carcinogenic, and excreted without excessive permanent accumulation in the tissues (Cahn and Haasen, 1992).

2.4. Release Kinetics

The release of active ingredients from controlled-release systems can follow a wide variety of patterns. However, the release kinetics from most systems that depend on membrane diffusion can be grouped into three release profiles:

- zero-order kinetics
- $t^{-1/2}$ kinetics
- first-order kinetics

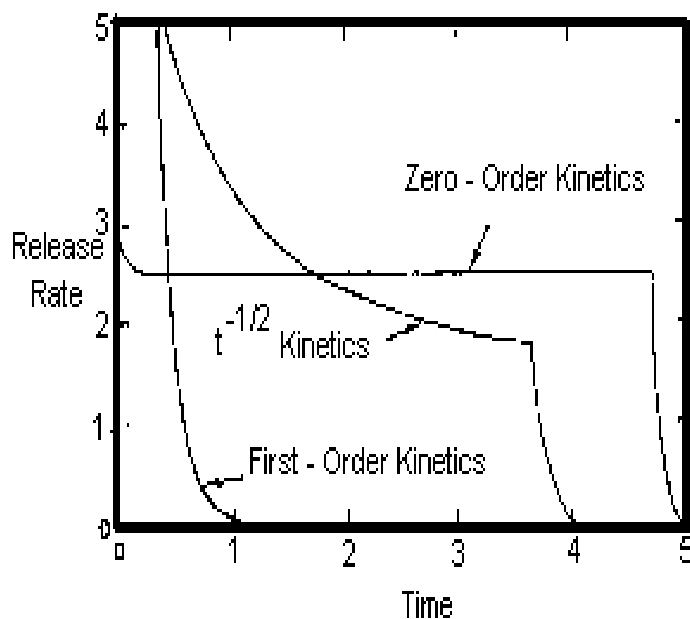


Figure 2.8. Comparison of release kinetics from conventional (first-order) and controlled-release formulations.

In zero-order kinetics, the release rate remains constant until essentially all of the active ingredient has been delivered. The term zero order that is a time-independent rate, derives from the release kinetics being independent of the quantity of drug remaining, i.e., drug concentration term raised zero power.

The release rate decreases proportionately to the square root of time in controlled-release systems with $t^{-1/2}$ kinetics (Smith and Herbig, 1992).

For systems exhibiting first-order kinetics, the release rate is proportional to the quantity of drug remaining in the system, i.e., proportional to the quantity to the first power, doubling the dose doubles the transfer rate.

The goal of a controlled release formulation is to improve the therapeutic value of the active drug component by reducing the ratio of the maximum and minimum plasma drug combination (C_{max}/C_{min}) while maintaining drug plasma levels within the therapeutic window. The controlled release form seeks to give a drug with sufficient frequency and dose so that the ratio C_{max}/C_{min} in plasma at steady state is less than the therapeutic index, and to maintain drug levels at constant effective concentrations. In principle, in order to keep a constant plasma drug level, the drug formulation should be

designed to provide an input rate into the body that is or approaches zero order, although in vivo profiles rarely match zero order kinetics based on in vitro models.

For both $t^{-1/2}$ and first-order systems most of the active ingredient is released during the first third of the total duration of release. Depending on the specifications for particular controlled-release formulations, either zero-order or $t^{-1/2}$ systems are typically preferred (Smith and Herbig, 1992).

CHAPTER 3

PREVIOUS STUDIES ON CONTROLLED-RELEASE SYSTEMS

3.1. Matrix Systems

The first study on matrix systems was conducted by Picker and Bikane (1998). They investigated the dependency of drug release from tablet formation and the factors influencing the microstructure of the tablet, such as densification, different particle size fractions, the dwell time during tableting and different drug concentrations. Their results show that it is only possible to produce a matrix tablet with cellulose acetate for controlled release applications by using longer dwell times. Without longer dwell times and the hydrostatic stress evolving during this process the bonding in the cellulose acetate matrix is dominated by hydrogen bonding which can be dissolved by the release medium.

Qiu et al. (1998) studied on the devices that consist of a hydrophobic middle layer and press-coated hydrophilic and/or hydrophobic barrier layer(s). The aim of producing such tablets was to overcome the inherent disadvantage of non-linear release associated with diffusion-controlled matrix devices by providing additional releasing surface with time to compensate for the decreasing release rate. In vivo release experiments were done using nine beagle dogs. At the end of the study they have concluded that zero-order or near zero-order release can be obtained using the proposed system designs which overcome the major disadvantage of nonlinear release associated with matrix devices.

Gren and Nyström (1999) prepared a multipleunit extended-release matrix by incorporating a hydrophilic drug (paracetamol) and lipophilic release modifiers (cetyl alcohol and paraffin) into porous cellulose matrices and they controlled the release rate by varying the ratio of cetyl alcohol to paraffin. The porosity of the matrix was found to increase during release due to formation of cracks and voids as cellulose swelled. Their results indicated that the rate of drug release is mainly controlled by diffusion through

the matrix but is also affected by the distribution of drug in the matrix and increase in porosity of the matrix.

Streubel et al. (2000) used two different polymers as matrix formers, the water insoluble and almost unswellable ethylcellulose (EC), and the water-soluble and highly swellable hydroxypropyl methylcellulose (HPMC). They proposed two different approaches to solve problem of pH-dependent release of weakly basic drugs. The first one is based on the addition of hydroxypropyl methylcellulose acetate succinate (HPMCAS, an enteric polymer), the second one is based on the addition of organic acids to the drug-polymer system. As a result they have found that the addition of HPMCAS to ethylcellulose-or HPMC- based matrix tablets failed to achieve pH-independent drug release, whereas the addition of organic acids to both matrix formers maintained low pH values within the tablets during drug release in phosphate buffer (pH 6.8 or 7.4) leading to pH-independent drug release.

3.2. Bioerodible Systems

Karasulu et al. (2000) investigated how various geometrical shapes such as triangle, cylinder, and half-sphere affect the release rate of theophylline from erodible hydrogel matrix tablets. They found that the release rate is highest from triangular tablets and lowest from cylindrical tablets.

3.3. Swelling Systems

Bettini et al. (1995) studied the swelling behavior and transport in swellable, ionic copolymers of 2-hydroxyethyl methacrylate and methacrylic acids for a wide range of copolymer compositions. The swelling behavior was determined by investigating the time -dependent change of the swelling and erosion front positions and associated gel layer as a function of the percentage of the ionic component (MAA). In addition, release of theophylline and metoclopramide-HCl were studied as a function of time. As a result they have found that the relatively rapid penetration of water established a water gradient within the hydrogel that led to a slower polymer swelling.

In another study, Bell and Peppas (1995) were measured the swelling force of interpolymer complexes as a function of time in various pH buffered solutions, and analyzed the results to determine the contributions of chain relaxation and diffusion on the swelling force. Their results indicated that chain relaxation is an important mechanism in the development of the swelling force.

To establish the relationship between front position and drug release kinetics Colombo et al (1996) studied on the movement of the penetrant and polymer fronts and the drug dissolution in highly loaded swellable matrix tablets. They confirmed that in swellable matrix tablets drug release rate is inversely proportional to the dynamics of gel layer thickness, which remains constant when the polymer is sufficiently soluble.

3.4. Membrane Systems

Liu et al. (2000a) studied with the sandwiched osmotic tablet system (SOTS), which is composed of a sandwiched osmotic tablet core surrounded by a cellulose acetate membrane with two orifices on both side of the surfaces for delivering nifedipine. They investigated the influences of tablet formulation variables, orifice size and membrane variables on nifedipine release from SOTS. As a result they found that two orifices with diameter ranging from 0.5 to 1.41 mm are suitable for the SOTS. Liu et al. (2000b) also studied with the monolithic osmotic tablet system, that consists of a monolithic tablet core coated with cellulose acetate membrane drilled with two orifices. The influences of tablet formulation variables including molecular weight and amount of polyethylene oxide, amount of potassium chloride, and amount of rice starch as well as nifedipine loading were investigated on drug release rate. They have found that both KCl and PEO had comparable positive effects, while the loading of nifedipine had a negative influence on drug release and they observed that the optimal orifice size was in the range of 0.25-1.41 mm and their results indicated that the hydrophilic plasticizer, PEG, improved drug release, whereas the hydrophobic plasticizer, triacetin, depressed drug release when they were incorporated in the CA membrane. Finally they have shown that monolithic osmotic tablet system was found to be able to deliver nifedipine at a rate of approximately zero-order up to 24 h, independent of both environmental media and agitation rate.

Graham et al. (1999) investigated the effect of formulation changes on the phase inversion dynamics and in vitro drug release properties of a PLGA-based drug delivery system by using optical microscopy, electron microscopy and high pressure liquid chromatography. Their results have shown that additives that accelerate the solution gelation rate at constant morphology result in high initial release rates, implying that drug diffusion through a tortuous two-phase gelled structure is faster than through a one-phase polymer solution. Conversely, additives that slow the rate of gelation dramatically reduce the initial drug release rate and lead to a more dense sponge like morphology.

Narisawa et al. (1995) studied on the factors affecting the in vivo drug release. They used theophylline and propranolol hydrochloride (PPL) as model drugs. Drug release behaviors from two multiple unit types of controlled release systems were observed in the gastrointestinal (GI) tract of beagle dogs. They concluded that with respect to drug release from controlled-release preparations coated with insoluble polymer based film coating, a good in vitro/in vivo correlation was observed in the early stages of drug release, irrespective of drug properties, but solubility of the drugs was found to be an important factor that affected the drug release in the lower site of GI tract of dogs.

Thombre et al. (1999a) demonstrated that the asymmetric membrane capsule can be used to deliver a poorly water soluble drug with a pH sensitive solubility such as glipizide. In order to obtain desired delivery duration, they solubilized the drug with the use of a pH-controlling excipient. Drug substances with a poor aqueous solubility were found to have very low rates, thus, the osmotic release rate of a drug from an asymmetric membrane capsule was found to depend on its solubility. They have shown that this limitation can be overcome for a drug such as glipizide, which has a pH-dependent solubility, by including a solubility modifying excipient in the capsule core.

In another study, Thombre et al. (1999b) describes a manual and a semi-automatic process developed for the manufacture of a novel non-disintegrating polymeric capsule. The capsule wall was made by a phase inversion process in which the membrane structure was precipitated on stainless steel mold pins by dipping the mold pins into a coating solution containing cellulose acetate-aceton-ethanol system.

In the following study, they used these capsules to describe the in vivo and in vitro drug release characteristics (Thombre et al., 1999c). They studied with phenylpropanolamine, chlorpheniramine, trimazosin and theophylline as model drugs. The results of kinetic studies have shown that the asymmetric membrane capsule has a higher permeability that is consistent with the asymmetric structure of the capsule wall.

Herbig et al. (1995) studied with asymmetric-membrane tablet coatings as in this study. They described the use of asymmetric-membrane coatings on pharmaceutical tablets. Trimazosin and doxazosin tablets were coated with cellulose acetate-acetone-formamide solution by dip-coating process and to demonstrate osmotic release, kinetic studies were conducted in water and $MgSO_4$ solutions. Kinetic studies were also conducted on tablets coated with dense membrane and results have shown that release rate from the asymmetric membrane coated tablets was about 65 times higher than the release rate from the dense coated tablets. They changed the coating thickness and have found that overall membrane thickness has no effect on release rates. In addition, they varied glycerol content (used as nonsolvent) in the membrane solution and observed that increasing glycerol content leads to an increase in number and size of the macropores in the skin layer.

CHAPTER 4

DIFFUSION IN ASYMMETRIC MEMBRANES

4.1. Diffusion in Dense Membranes

Transport through dense polymeric membranes in controlled-release systems occurs by a solution-diffusion process that is called as passive diffusion. The active agent must first dissolve in the membrane and then diffuse from the surface of high active ingredient concentration to the surface of low concentration.

The active ingredient exists in a highly saturated state within the reservoir and is able to diffuse through the membrane in response to a gradient in thermodynamic activity. As long as the solution within the reservoir is saturated and sink conditions are maintained at the releasing film interface, the concentration gradient across the membrane remains constant and release of the drug follows zero-order kinetics (Cahn and Haasen, 1992).

As a drug particle undergoes dissolution, the drug molecules on the surface are the first to enter into solution creating a saturated layer of drug-solution which envelopes the surface of the solid drug particle. This layer of solution is referred to as the diffusion layer. From this layer, the drug molecules pass throughout the dissolving fluid and make contact with the membranes. As the molecules of drug continue to leave the diffusion layer, the layer is replenished with dissolved drug from the surface of the drug particle (Ansel and Popovivch, 1990).

4.2. Diffusion in Asymmetric Membranes

The solution diffusion model described in Section 4.1 is easy to understand and valuable in practice. However, in asymmetric type membranes, mechanisms of the transport of components are much more complex. In a simple manner, asymmetric membranes can be regarded as a dual-zone system, consisting of very thin skin layer and a much thicker, porous sublayer. Usually, the transport mechanism of the skin is

assumed to obey the solution-diffusion model, whereas the porous support layer is considered as a system of capillaries arranged in parallel.

Transport of molecules through the asymmetric membrane is influenced both by the transport resistance in the skin layer and the porous substrate. Simplified, the basic equation for mass transport of a permeating component in the asymmetric membrane can be written as follows;

$$Rate = D_{eff} A \frac{C_1 - C_2}{L} \quad (4.1)$$

This equation is derived based on the assumption that steady-state condition is achieved in the membrane. Then, the concentration profile within the membrane is linear and time independent. Effective diffusivity, D_{eff} , in equation 4.1 takes into account the presence of the pores and, thus, tortuous diffusional path that permeating molecules should follow. Concentration of permeating molecule at the boundaries of the membrane C_1 and C_2 , can be related to the concentration within the surrounding medium through a linear equilibrium relationship as follows;

$$C_1 = KC_1^* \quad C_2 = KC_2^* \quad (4.2)$$

If equation 4.2 is inserted into equation 4.1, then

$$Rate = D_{eff} KA \frac{(C_1^* - C_2^*)}{L} \quad (4.3)$$

where, the product of the effective diffusivity of the solute across the membrane, D_{eff} , and the partition coefficient of the solute between the membrane and the adjacent phase, K , is defined as the effective permeability of the membrane, P_{eff}

$$P_{eff} = D_{eff} K \quad (4.4)$$

The effect of the transport resistance of dense skin layer and the porous sublayer on permeation characteristics can be demonstrated by the resistance model which was first demonstrated by Henis and Tripodi (1992). According to this model, the mass flow can be considered analogous to an electrical flow in a circuit consisting of three resistance components in a series-parallel configuration as shown in Figure 4.1.

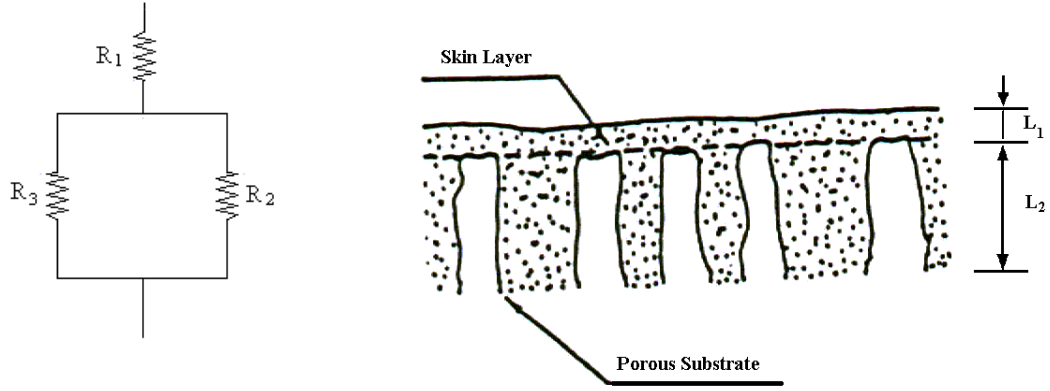


Figure 4.1. Schematic cross section of an asymmetric membrane and the mass transport resistance configuration.

The overall permeation resistance R_t is given by

$$R_t = R_1 + R_2 R_3 / (R_2 + R_3) \quad (4.5)$$

where R_1 is the resistance of the skin layer; R_2 and R_3 are the resistances of the pores and the polymer matrix, respectively. These resistances can be written as

$$R_1 = \frac{L_1}{P_{eff1} A} \quad (4.6)$$

$$R_2 = \frac{L_2}{P_{eff2} A \varepsilon} \quad (4.7)$$

$$R_3 = \frac{L_2}{P_{eff1} A (1 - \varepsilon)} \quad (4.8)$$

where L_1 and L_2 are the thickness of the skin layer and the substrate, respectively; $P_{eff,1}$ and $P_{eff,2}$ are the effective permeability coefficients through the polymer matrix and the pores, respectively and ε is the area porosity of the substrate.

4.3. Diaphragm Cell Model

The permeability of porous membranes can be determined using the diaphragm cell model (Cussler, 1997). In this model, it is assumed that the steady-state condition is reached in the membrane even though concentrations in the adjacent compartments

change with time. This is a reasonable assumption since the membrane has a much smaller volume than the adjacent compartments. In this steady state, the rate of mass transfer across the membrane is given by equation 4.3. If the adjacent compartments next to upper and lower side of the membrane are referred to as donor and receiver compartments and corresponding concentrations are denoted as C_D and C_R , respectively, then equation 4.3 is rewritten as follows;

$$Rate = P_{eff} \frac{A}{L} (C_D - C_R) \quad (4.9)$$

The overall mass balances on the donor and receiver compartments are as follows;

$$V_D \frac{dc_D}{dt} = -P_{eff} \frac{A}{L} (C_D - C_R) \quad (4.10)$$

$$V_R \frac{dc_R}{dt} = P_{eff} \frac{A}{L} (C_D - C_R) \quad (4.11)$$

where V_D and V_R are the liquid volumes in the donor and receiver compartments, respectively, (cm^3), t is time (s) and A is the surface area of the membrane. If equation 4.11 is subtracted from equation 4.10, then,

$$\frac{d}{dt} (c_D - c_R) = -P_{eff} \beta (c_D - c_R) \quad (4.12)$$

where β is a geometric constant characteristic of the diffusion cell, defined as

$$\beta = \frac{A}{L} \left[\frac{1}{V_D} + \frac{1}{V_R} \right] \quad (4.13)$$

The differential equation is subjected to the initial condition

$$\text{at } t=0, \quad c_D - c_R = c_D^0 - c_R^0 \quad (4.14)$$

where, c_D^0 and c_R^0 are the initial concentrations in the donor and receiver, respectively. Integrating the flux equation subject to this initial condition gives the result

$$\ln \left(\frac{c_D^0 - c_R^0}{c_D - c_R} \right) = P_{eff} \beta t \quad (4.15)$$

If it is assumed that there is no accumulation in the membrane,

$$m_{tot} = c_D^0 V_D + c_R^0 V_R = c_D V_D + c_R V_R \quad (4.16)$$

and combining equations 4.15 and 4.16, functional time dependence of the concentrations in the donor and the receiver can be obtained as follows (Ristic, 2000).

$$c_D = \frac{c_D^0}{\left(1 + \frac{V_R}{V_D}\right)} + \frac{1}{1 + \frac{V_D}{V_R}} \left[c_R^0 + (c_D^0 - c_R^0) \exp(-P_{eff} \beta t) \right] \quad (4.17)$$

$$c_R = \frac{c_R^0}{\left(1 + \frac{V_D}{V_R}\right)} + \frac{1}{1 + \frac{V_R}{V_D}} \left[c_D^0 - (c_D^0 - c_R^0) \exp(-P_{eff} \beta t) \right] \quad (4.18)$$

CHAPTER 5

STATISTICAL DESIGN AND ANALYSIS OF EXPERIMENTS

Experimental design is an important tool in engineering for improving the performance of a manufacturing process. The use of experimental design can result in products, which are easier to manufacture, products that have enhanced field performance and reliability, lower product cost, and shorter product design and development time.

Statistical design of experiments refers to the process of planning the experiment. Collected appropriate data can be analyzed by statistical methods, resulting in valid and objective conclusions. If meaningful conclusions from the data are desired, the statistical approach is necessary. When the problem involves data that are subject to experimental errors, statistical methodology is the only objective approach to analysis. Thus, there are two aspects to any experimental problem: the design of the experiment and the statistical analysis of the data. These two parts are related because the method of analysis depends on the design employed.

The first step in the design of any experiment is determining which factors affect the response in a characterization experiment. A logical next step is to optimize, that is, to determine region in the important factors that leads to the best possible response.

5.1. Experimental Designs for Fitting Response Surfaces

Response surface methodology is commonly used and very useful for the modeling and analysis of problems in which response is influenced by several variables, and, the objective is to optimize the response. If y denotes the response affected by “ k ” parameters, then,

$$y = f(x_1, x_2, \dots, x_k) + \varepsilon \quad (5.1)$$

where ε represents the noise or error observed in the response y . If the expected response $E(y) = f(x_1, x_2, \dots, x_k) = \eta$, then the surface represented by

$$\eta = f(x_1, x_2, \dots, x_k) \quad (5.2)$$

is called as a response surface. The proper choice of an experimental design plays an important role in fitting and analyzing response surfaces. The suitable experimental design should

- a) provide a reasonable distribution of data points
- b) allow experiments to be performed in blocks
- c) allow new designs of higher order, i.e., allow to increase number of experiments
- d) does not require large number of experimental runs
- e) allow to fit data to known models
- f) provide precise estimates of the model coefficients
- g) does not require too many levels of independent variables

There are many response surface design methods available in the literature. In all these techniques, the idea is to generate the design points that are equidistant from a specified origin. A brief summary of design techniques is listed below: (Montgomery, 2001).

1)The orthogonal first-order design:

This type of designs include the 2^k factorial and fractions of the 2^k series in which k is the number of design variables. The data is fitted to first order model.

2)The central composite design (CCD):

It is a very efficient design for fitting the second-order model. Depending on the geometric shape of the region of interest, variations of the central composite design such as phase-central composite design or the phase-centered cube or the Box-Behnken design are used.

3)Computer-generated (optimal) design:

If the experimental region is not either a cube or a sphere, then standard response surface designs will not be applicable. In these cases, computer-generated designs are usually used.

4)Robust parameter design:

In this approach, the variables in a process or product are classified as either control (controllable) variables or noise (or uncontrollable) variables. The settings for the controllable variables are found that minimize the variations transmitted to the response from the uncontrollable variables.

5) Mixture design:

This type of design is used when all variables influencing the response are not independent and will be discussed in detail in the next section.

5.2. Mixture Design

In some experimental situations the factors cannot be varied independently of each other. Many products are manufactured by mixing together two or more ingredients or components.

In mixture experiments, the factors are the components or ingredients of a mixture, and consequently their levels are not independent. For example, if x_1, x_2, \dots, x_p denote the proportions of p components of a mixture, then

$$0 \leq x_i \leq 1 \quad i=1,2,\dots,p \quad (5.3)$$

and

$$x_1 + x_2 + \dots + x_p = 1 \quad (\text{i.e., 100 percent}) \quad (5.4)$$

For a two-component system, the mixture space is a rectangle, while, with three components, the mixture space is a triangle with vertices corresponding to pure components.

When there is no constraint on the individual components in the mixture, simplex designs are used to study the effects of mixture on components on the response variable. If the mixture contains p components and the experimental design points take $m+1$ equally spaced values from 0 to 1, then

$$X_i = 0, \frac{1}{m}, \frac{2}{m}, \dots, 1 \quad i=1,2,\dots,p \quad (5.5)$$

In general, the number of points in a $\{p,m\}$ simplex lattice design is

$$N = \frac{(p+m-1)!}{m! (p-1)!} \quad (5.6)$$

Figure 5.1 shows the experimental design points in a $\{3,3\}$ simplex lattice.

In some mixture problems, constraints on the individual components arise. If there is only lower bound constraint

$$\ell_i \leq x_i \leq 1 \quad i=1,2,\dots,p \quad (5.7)$$

simplex design can still be used by defining pseudocomponents, defined as

$$x'_i = \frac{x_i - \ell_i}{\left(1 - \sum_{j=1}^p \ell_j\right)} \quad (5.8)$$

with $\sum_{j=1}^p \ell_j < 1$. Then sum of compositions of pseudocomponents is equal to 1, $\sum_{i=1}^p x'_i = 1$.

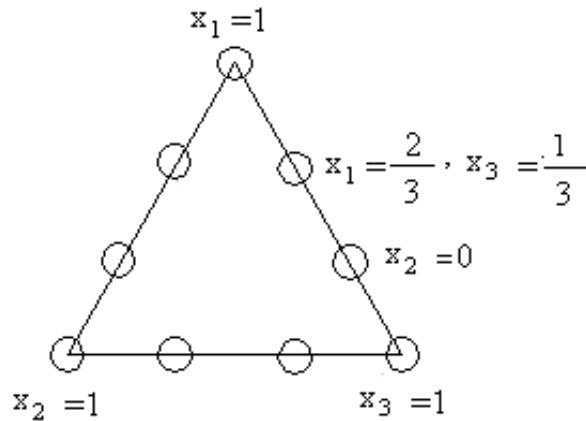


Figure 5.1. Simplex lattice design for a ternary mixture.

If the components have both upper and lower bound constraints, then the design does no longer have a standard shape. For these types of mixture problems, computer generated designs are used.

5.3. Mixture Models

Mixture models are usually different from the usual polynomials employed in fitting the response surface of other design problems. Mixture models commonly used in the literature are listed as follows.

Linear

$$y = \sum_{j=1}^q b_j x_j \quad (5.9)$$

Quadratic

$$y = \sum_{j=1}^q b_j x_j + \sum_{i=1}^{q-1} \sum_{j=i+1}^q b_{ij} x_i x_j \quad (5.10)$$

Special Cubic

$$y = \sum_{j=1}^q b_j x_j + \sum_{i=1}^{q-1} \sum_{j=i+1}^q b_{ij} x_i x_j + \sum_{i=1}^{q-2} \sum_{j=i+1}^{q-1} \sum_{k=j+1}^q b_{ijk} x_i x_j x_k \quad (5.11)$$

Cubic

$$y = \sum_{j=1}^q b_j x_j + \sum_{i=1}^{q-1} \sum_{j=i+1}^q b_{ij} x_i x_j + \sum_{i=1}^{q-1} \sum_{j=i+1}^q C_{ij} x_i x_j (x_i - x_j) + \sum_{i=1}^{q-2} \sum_{j=i+1}^{q-1} \sum_{k=j+1}^q b_{ijk} x_i x_j x_k \quad (5.12)$$

CHAPTER 6

EXPERIMENTAL

In this thesis experimental study consists of five parts:

- Tablet preparation
- Tablet coating
- Dissolution studies
- Permeability studies
- Characterization

And this chapter discusses the details of experimental procedures.

6.1. Properties of Polymer and Model Drug

Throughout this study, theophylline anhydrate and cellulose acetate were used as a model drug and membrane forming polymer respectively. Theophylline anhydrate was kindly supplied by Eczacıbaşı A.Ş.

Theophylline is structurally classified as a methylxanthine. It occurs as a white, odorless, crystalline powder with a bitter taste. Figure 6.1 shows the crystalline structure of theophylline. Anhydrous theophylline has the chemical name 1H-Purine-2, 6- dione, 3, 7 –dihydro-1, 3- dimethyl.

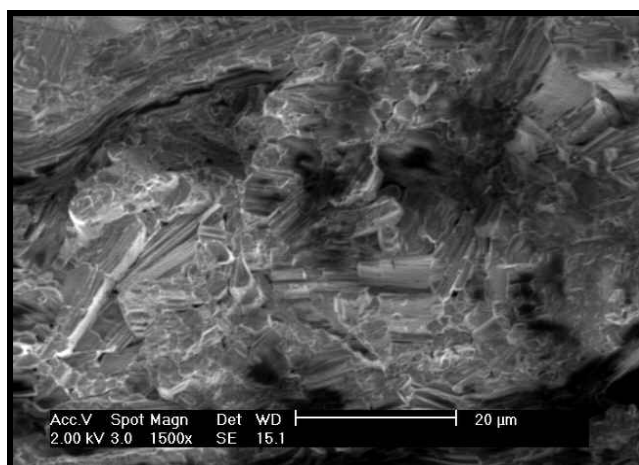


Figure 6.1. SEM picture of crystalline theophylline anhydrate.

1 g of theophylline dissolves in 120 ml of water. Anhydrate form is more soluble than hydrate form (Karasulu, 1996). The molecular formula of anhydrous theophylline is $C_7H_8N_4O_2$ with a molecular weight of 180.17 and molecular structure is shown in Figure 6.2.

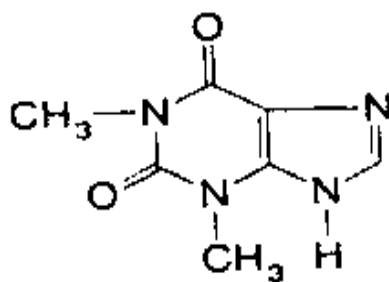


Figure 6.2. Molecular structure of theophylline.

Theophylline is used for the treatment of the chronic asthma and other chronic lung diseases symptoms and reversible airflow obstruction.

Cellulose acetate that is an ester of cellulose and acetic acid, is white, odorless and non-toxic, natural thermoplastic polymer. Figure 6.3. shows the molecular structure of the cellulose.

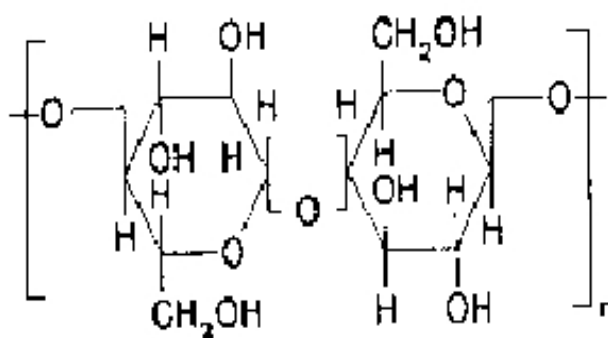


Figure 6.3. Molecular structure of cellulose.

Cellulose acetate is the generic term used to describe a variety of acetylated cellulose polymers. This includes cellulose diacetate, cellulose triacetate and the mixed esters of cellulose acetate propionate and cellulose acetate butyrate. Cellulose diacetate and cellulose triacetate are acetylated on one, two or all three of the available sites on each glycopyranose ring. The degree of substitution, along with the solvents used during the manufacturing process, determine the composition and properties of the acetate produced.

6.2. Tablet Preparation

Tablets are solid dosage forms of medicinal substances usually prepared with the aid of suitable pharmaceutical adjuncts. Tablets may vary in size, shape, weight, hardness, thickness, disintegration characteristics, and in other aspects, depending upon their intended use and method of manufacture.

In this study, tablets were prepared by compressing powder form of the drug with the use of hydraulic press operated at 110 MPa pressure. Stainless steel die with a diameter of 1.2 cm was used to produce 400 mg drug tablets having cylindrical shapes.

6.3. Tablet Coating

6.3.1. Preparation of Membrane Solution

Tablets prepared by compression of drug were coated with ternary solution consisting of polymer, solvent and nonsolvent. Polymer is completely soluble in solvent and has partial solubility in nonsolvent. Membrane solutions were prepared by completely dissolving the polymer in solvent and then adding nonsolvent to the homogeneous binary mixture. Tablets were coated with different solutions prepared by dissolving cellulose acetate in

- a) different nonsolvents with the same polymer-solvent and nonsolvent ratios,
- b) the same solvent and nonsolvent with different polymer-solvent and polymer-nonsolvent ratios.

The properties of chemicals and their compositions used in the preparation of membrane solutions are given in Table 6.1.

Table 6.1. Properties of chemicals used for drug-release experiments.

Materials	Specifications
Cellulose Acetate	39.7 wt % acetyl content Average M_n 50,000 (GPC) Aldrich
Acetone (CH_3COCH_3)	99% , $M= 58.08 \text{ g/mol}$, $d= 0.79 \text{ kg/l}$ Merck
Formamide (HCONH_2)	99.5% , $M= 45.04 \text{ g/mol}$, $d= 1.13 \text{ kg/l}$ Merck
1- Octanol ($\text{C}_8\text{H}_{18}\text{O}$)	99%, $M= 130.23 \text{ g/mol}$, $d= 0.83 \text{ kg/l}$ Merck
Potassium Dihydrogen Phosphate (KH_2PO_4)	$M= 136.09 \text{ g/mol}$ Merck
Sodium Hydroxide Pellets (NaOH)	$M= 40.00 \text{ g/mol}$ Merck
1-Hexanol ($\text{CH}_3(\text{CH}_2)_5\text{OH}$)	98%, $d= 0.814 \text{ kg/l}$ Aldrich
Glycerol	87%, $d= 1.23 \text{ kg/l}$ Merck
Phosphoric Acid (H_3PO_4)	85.2% Sigma

6.3.2. Dip-Coating

Tablets were coated by dipping them in the polymer solution followed by rotation and drying in ambient conditions. The coating process places a thin tight coating over the compressed tablets.

6.4. Dissolution Studies

The process by which a drug particle dissolves is termed dissolution and the rate at which it dissolves in medium is referred to as its dissolution rate. Dissolution testing is used in product development to assist in selection of a candidate formulation, in research to detect the influence of critical manufacturing variables such as binder effect,

mixing effect, coating parameters, types of drug, and as a quality control procedure in pharmaceutical production.

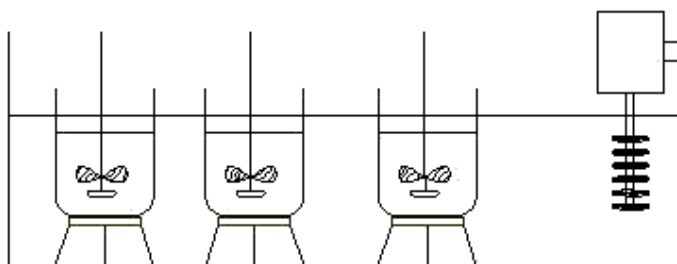


Figure 6.4. Dissolution test apparatus.

In this study, the *in vitro* dissolution studies were performed using the United States Pharmacopeia XXIII (USP XXIII) dissolution methodology. According to this standard, 900 ml of dissolution medium was placed in the vessel and temperature was allowed to come 37 °C using a constant temperature bath. Then, the single tablet to be tested was immersed in the vessel and the solution was stirred with a mixer adjusted at 50 rpm. The dissolution test apparatus was designed according to USP standards and is shown in Figure 6.4.

Under normal circumstances, a drug may be expected to remain in stomach for 2 to 4 hours (gastric emptying time) and in the small intestines for 4 to 10 hours. The pH of the stomach varies from 1 to 3 and in ascending colon this value is between pH 7 and pH 8. To simulate actual dissolution environment in the body, the pH of the dissolution medium was kept at 3 during the first 3.5 hours of dissolution test, then, it was increased to 7.4 and was kept at that value until the end of the test. In the preparation of the dissolution medium, 8.5 v% phosphoric acid was added to the 900 ml distilled water to reduce pH to the value of 3. After 3.5 hours, the pH of the medium was increased to 7.4 by adding 5.3 M NaOH to the solution. During 5 hours of dissolution test, samples were taken from the dissolution medium at certain times and concentration of drug in the release medium was determined by spectrophotometer (Shimadzu, UV-1601). The peak for theophylline anhydrate is observed at 272 nm wavelength. Each dissolution test was conducted on three tablets and the mean of the results was calculated. The UV spectrum

and the calibration curves of theophylline anhydrate prepared in three different solutions are shown in Appendix A and B in Figures A1 through B3, respectively.

6.5. Permeability Studies

To investigate the permeation characteristics of membranes, diffusion cell shown in Figure 6.5 was designed. The diffusion cell consists of two compartments, the upper one is a donor compartment and the lower one is a receiver compartment.

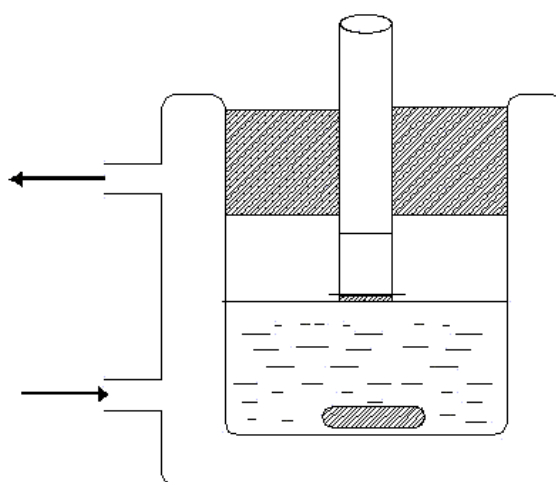


Figure 6.5. Schematic representation of diffusion cell.

The glass tube with a diameter of 2.5 cm acts as the donor compartment while the beaker with a diameter of 8 cm acts as the receiver compartment. The position of the glass tube in the beaker is fixed using rubber plugs. The membrane is tightly sealed at the bottom of the glass tube, which has open ends. A constant temperature is maintained during the experiment by means of water circulation in the jacket surrounding the beaker. Mixing in the receiver compartment is provided by magnetic stir bar. During the experiment, the donor compartment is filled with 10 ml theophylline solution with an initial concentration of 7 mg/ml while the receiver compartment is filled with 50 ml phosphate buffer solution with a pH of 3. Temperature in both compartments is kept constant at 37 °C. During 5 hours, 10 µL samples were taken periodically from both

compartments to monitor the change in drug concentration with time. Concentration of theophylline was determined using UV spectrophotometer.

6.6. Characterization

In this part of the study the morphology of the casted films was investigated by scanning electron microscopy (Philips, XL-30SFG) and the phase analysis was conducted by using the program analySIS 2.1 of scanning electron microscopy system. The gray level difference between polymer matrix and the pores were used. Each phase was represented by different gray level and according to these different gray values the percentage of each phase was calculated by the program.

CHAPTER 7

RESULTS AND DISCUSSION

This chapter was divided into three parts that covers the results of the dissolution studies, along with morphological studies, permeability studies and statistical analysis. In dissolution studies, drug release rates from the asymmetric and dense membrane coated tablets were compared to assess the performance of asymmetric membranes. The effects of polymer/solvent (P/S), polymer/nonsolvent (P/NS) and solvent/nonsolvent (S/NS) ratios, number of coating layer, coating time, and evaporation conditions on release rate of the drug were investigated. Additionally, different types of nonsolvents were tried in the preparation of membrane solutions and their effects on release rate were compared.

In permeability studies, permeation characteristics of the membranes cast from ternary solutions were investigated. The results of statistical analysis were shown both in tabular and graphical form, which allow to determine optimum response in the design area.

In morphological studies, scanning electron microscope (SEM) pictures of different types of membranes were analyzed to determine overall thickness, skin layer thickness, pore sizes and porosity.

7.1. Dissolution and Morphological Studies

Dissolution studies on tablets coated with asymmetric type membranes were conducted to determine the release rate of drug, as well as the release kinetics. For this purpose, the graph of concentration of drug in the dissolution medium as a function of time was analyzed by fitting the experimental data to a linear equation of the form $y = ax$. The release rate of theophylline was calculated by multiplying the slope of the linear line (a) with the volume of the dissolution medium. The regression coefficient, R^2 , indicates the accuracy or perfectness of linear fit to the experimental data. The release rate of theophylline from tablets coated with membrane solutions consisting of cellulose

acetate (CA), acetone (Ac), water (W) and corresponding R² values are tabulated in Table 7.1.

Table 7.1. Release rates and characterization of membranes prepared for dissolution studies.

Composition			Porosity (%)	Total Thickness (μm)	Skin Thickness (μm)	Average Pore Size (μm)	Release Rate (mg/min)	R ²
CA	Ac	W						
10	90	0	Dense	8.40	-	0.383	0.0090	0.9802
10	80	10	22.33	16.05	1.14	1.040	0.0630	0.9454
5	80	15	27.40	10.52	0.63	0.885	0.1800	0.9752
15	80	5	16.48	15.27	5.00	0.670	0.0036	0.9607
5	85	10	26.09	133.95	-	19.925	0.1800	0.9963
15	75	10	33.00	20.06	1.85	1.110	0.0180	0.9893
15	70	15	28.44	34.91	2.58	1.220	0.0081	0.9978
3	80	17	34.19	13.69	-	1.100	0.7200	0.9700
5	90	5	-	6.46	-	0.970	0.2700	0.9500
10	85	5	-	13.13	-	-	0.0450	0.9755
10	75	15	56.24	30.32	0.61	1.160	0.0540	0.9962

One of the goals in developing a controlled release system is to provide zero-order release kinetics since, in this case, the release rate remains constant, independent of drug remaining as shown in equation 7.1.

$$\frac{dC}{dt}V = \frac{dm}{dt} = kC^0 = \text{constant} \quad (7.1)$$

According to equation 7.1, the requirement to obtain zero-order release kinetics is to observe a linear release profile with respect to time. This goal was reached for all tablet coatings prepared in this study since R² values close to one obtained for each dissolution experiment indicate linear relationship between concentration of drug in the dissolution medium and time.

Morphological studies were conducted on films cast from solutions having the same compositions as those used in coating the tablets. Initial casting thickness of all the membranes is 300 μm. SEM pictures of these films were taken to determine overall thickness, skin layer thickness, average pore sizes as well as the porosity. In these pictures, gray parts represent the polymer matrix, while the black parts are porous

regions. Phase analyses were conducted by using analySIS 2.1 and the results were shown in Table 7.1.

The results of dissolution studies and phase analysis were used to calculate resistances of the skin layer and the substrate as well as the individual resistances of the polymer matrix and the pores in the substrate. The values are listed in Table 7.2. It can be noticed from equation 7.2 that the ratio of total resistance of dense coating ($R_{total, dense}$) to that of the asymmetric coating ($R_{total, asymmetric}$) is equal to the ratio of release rate of asymmetric membrane to the release of dense membrane.

$$\frac{R_{total, dense}}{R_{total, asymmetric}} = \frac{Rate_{asymmetric}}{Rate_{dense}} \quad (7.2)$$

The total resistance of dense coating was calculated from equation 7.3 using experimentally measured permeability as well as the thickness and area of the membrane.

$$R_{total, dense} = \frac{L_{total}}{P_{dense} Area} \quad (7.3)$$

Then, total resistance of asymmetric coating was calculated from equation 7.2 using release rates listed in Table 7.1.

Table 7.2 Calculated resistances of skin layer, substrate, polymer and pores of the membranes

Composition			R_{skin}	$R_{substrate}$	$R_{polymer}$	R_{pore}
CA	Ac	W				
10	80	10	32.6	1.7	548.6	1.7
5	80	15	18.0	*	389.3	*
15	80	5	142.9	457.2	351.4	*
5	85	10	40.0	*	5124.9	*
15	75	10	52.9	67.2	776.7	73.5
15	70	15	73.7	193.0	1291.0	226.9
3	80	17	*	3.0	594.5	3.0
5	90	5	*	8.0	184.6	8.4
10	85	5	*	48.0	375.2	55.1
10	75	15	17.4	22.6	1940.1	22.8

* These values could not be calculated.

The effect of skin layer and substrate resistances on the total resistance was ascertained using the resistance model discussed in Chapter 4. According to this model, the

resistance of skin layer (R_{skin}) was determined from equation 4.6 and the resistance of substructure was calculated by subtracting the skin layer resistance from the total resistance. The resistances of the pores (R_{pore}) and polymer matrix (R_{polymer}) in the porous substrate were calculated using equation 4.7 and 4.8, respectively.

7.1.1. Comparison of the Drug Release Rates of Dense and Asymmetric Membrane Coated Tablets

Dissolution kinetics of the dense and the asymmetric-membrane coated tablets were determined to compare the drug release rates of these membranes. The dense coating was applied by dip-coating the tablet in a solution consisting of 10% cellulose acetate dissolved in acetone, whereas the asymmetric coating was obtained by dipping the tablet in a solution consisting of 10% cellulose acetate, 80% acetone and 10% water. The release profiles for both types of coated tablets are shown in Figure 7.1.

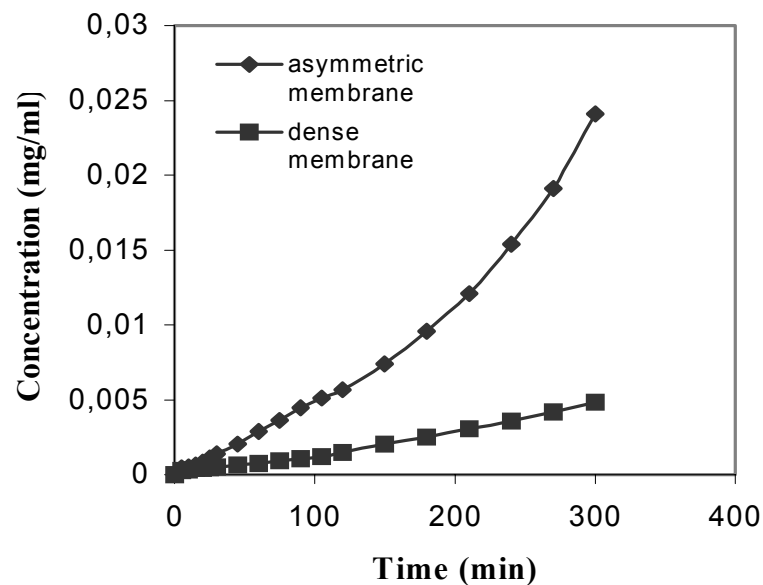


Figure 7.1. Release of theophylline from tablets coated with dense and asymmetric-membrane coatings.

The release rate from the asymmetric-membrane coated tablet was about 7 times higher than the release rate from the dense-coated tablet. This is due to the fact that in dense-coating, diffusional resistance to transport of the drug occurs through the overall

thickness while in asymmetric coating most of the resistance to transport is in the thin skin rather than in the porous substrate. Higher drug release rate from asymmetric membrane coating is expected when SEM pictures of these two types of membranes shown in Figure 7.2 and Figure 7.3 are compared.

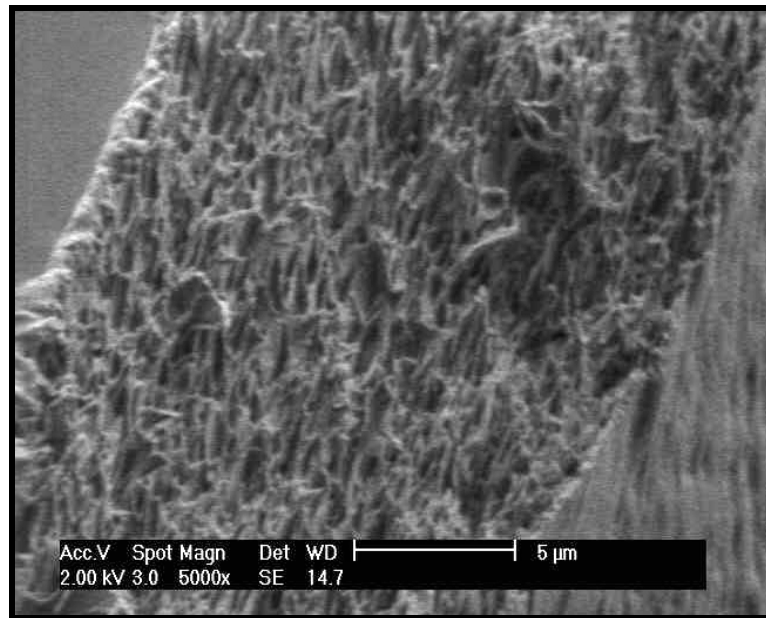


Figure 7.2. SEM picture of cross section of a membrane. Initial composition: 10% CA, 80% Acetone, 10% Water. Magnificationx5000.

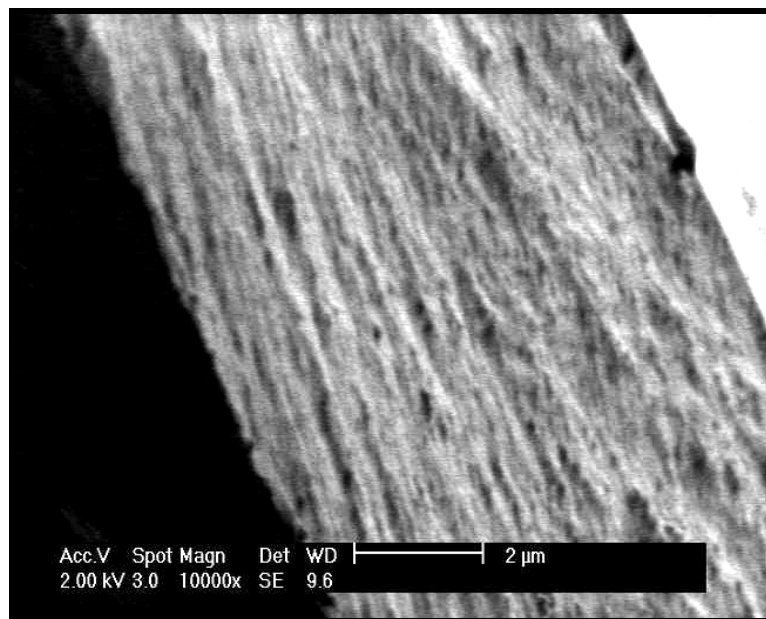


Figure 7.3. SEM picture of cross section of a membrane. Initial composition:

10% CA, 90% Acetone. Magnificationx10000.

Figure 7.2 indicates that membrane cast from ternary solution of polymer (CA), solvent (acetone) and nonsolvent (water) has an asymmetric structure. In this figure, dense layer is facing to the top of the picture while porous layer is at the bottom. Porous layer has a sponge like structure and pores are interconnected. This is a desired structure since it leads to high permeabilities. The overall thickness of the membrane is 16.05 μm while the thickness of the skin layer is only 1.14 μm . The porosity and average pore size were determined as 22.3% and 1.04 μm , respectively.

The membrane cast from binary mixture of CA and acetone has a dense symmetric structure as shown in Figure 7.3. The average total thickness and the average pore size were determined as 8.4 μm and 0.383 μm , respectively. Pores in the asymmetric membrane are almost three times larger than those in dense membrane. Thus, the substrate resistance of the asymmetric membrane is only 5% of the total resistance calculated from the ratio of $R_{\text{substrate}}/R_{\text{total}}$ and mass transport of drug molecules is mainly controlled by diffusion in thin skin layer that is only 7.1% of the total thickness. Since the thickness of skin layer of the asymmetric membrane is smaller than the overall thickness of the dense membrane, lower drug release rate was obtained from dense membrane.

7.1.2. Effect of Polymer / Solvent (P/S) Ratio on Release Rate

To investigate the effect of polymer-solvent ratio (P/S) on drug release rate, tablets were coated with solutions consisting of three different nonsolvent composition which are 5% water and 15/80, 5/90 and 10/85 P/S ratios, 10 % water and 5/85, 10/80, 15/75 P/S ratios and finally 15% water and 5/80, 15/70 and 10/75 P/S ratios.

The release rate of theophylline as a function of P/S ratio for three different nonsolvent compositions is shown in Figure 7.4.

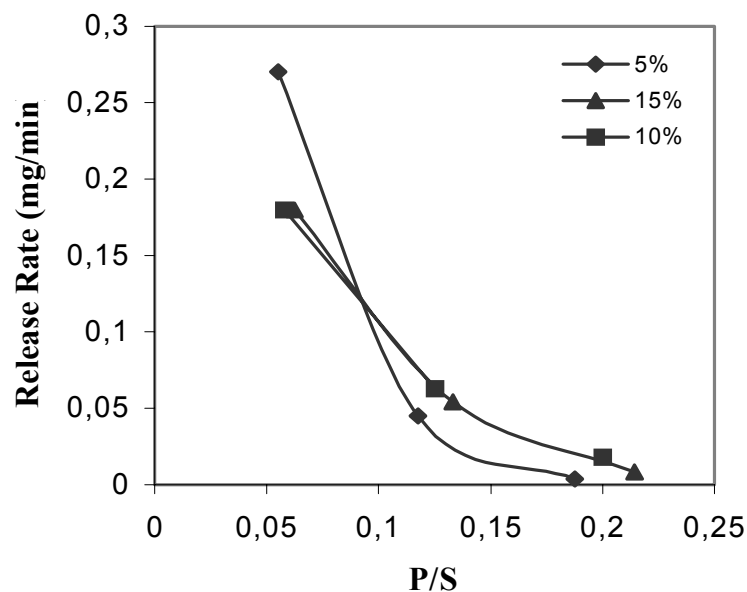


Figure 7.4. Release rate of theophylline as a function of P/S ratios for 5% 10% and 15% water content.

The release rates of tablets prepared from 5% water decreases exponentially with increasing P/S ratios, due to increasing resistance to transport of theophylline molecules and the change in morphology of the membranes. With decreasing P/S ratio the change in morphology from a dense structure to a porous one was observed from SEM pictures as shown in Figure 7.5 through 7.7.

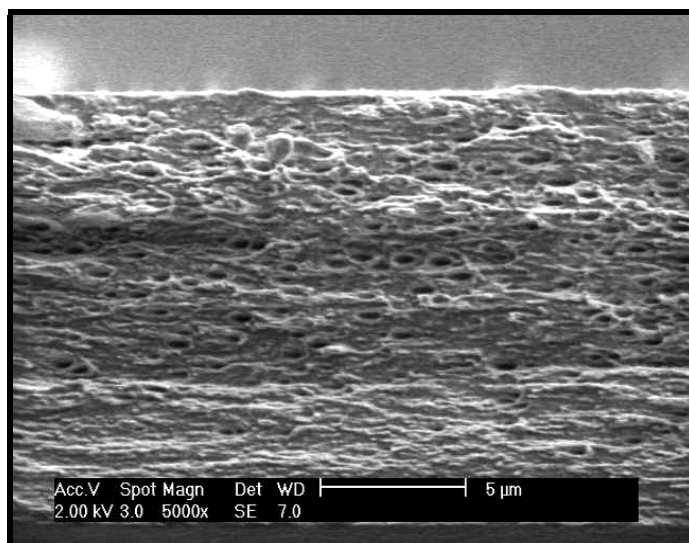


Figure 7.5. SEM picture of cross section of a membrane. Initial composition: 15% CA, 80% Acetone, 5% Water. Magnificationx5000.

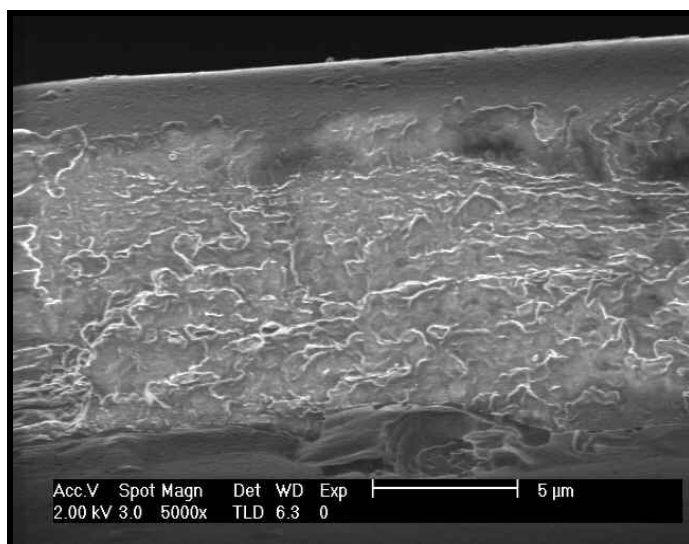


Figure 7.6. SEM picture of cross section of a membrane. Initial composition: 10% CA, 85% Acetone, 5% Water. Magnificationx5000.

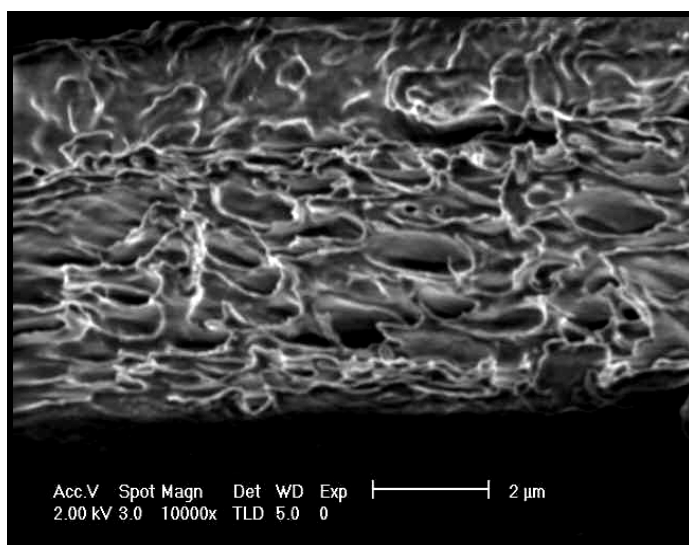


Figure 7.7. SEM picture of cross section of a membrane. Initial composition: 5% CA, 90% Acetone, 5% Water. Magnificationx10000.

The membrane prepared from the solution having highest P/S ratio (15/80) and the lowest drug release rate has the highest total and skin layer thickness, 15.27 μm and 5 μm, respectively, because of the high polymer concentration. Figure 7.7 indicates that membrane prepared from low polymer concentration (P/S = 5/90) has a porous structure

in which sponge like cylindrical pores with a wide pore size distribution was observed.

The release rate of membranes prepared from solutions including 10% and 15% water also decreases with increasing P/S ratio. SEM picture of the membrane prepared from the lowest P/S ratio of 5/85 is shown in Figure 7.8.

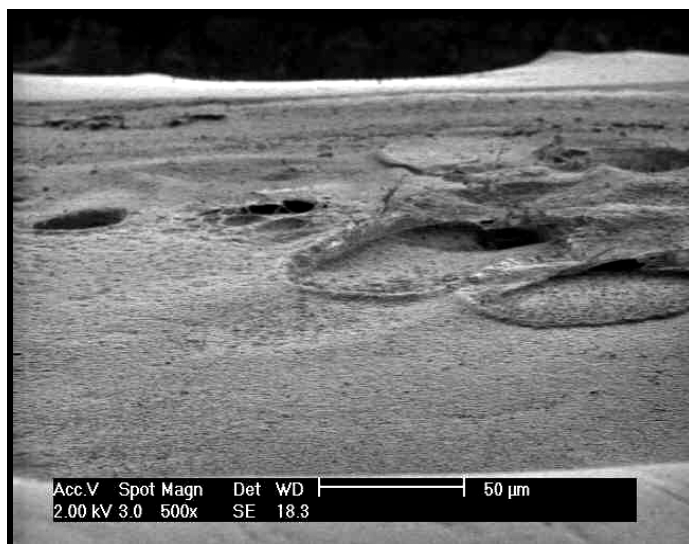


Figure 7.8. SEM picture of cross section of a membrane. Initial composition: 5% CA, 85% Acetone, 10% Water. Magnificationx500.

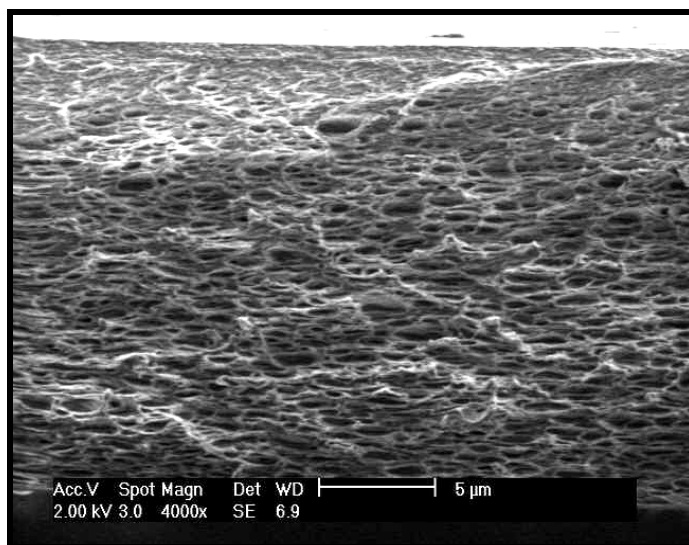


Figure 7.9. SEM picture of cross section of a membrane. Initial composition: 15% CA, 75% Acetone, 10% Water. Magnificationx4000.

The total thickness of this membrane, 133.9 μm , is much higher than the thickness of other membranes due to the presence of macropores having average size of 19.9 μm . The average pore size of the pores at the bottom of the picture corresponding to dense skin layer decreases to 630 nm. This membrane has the highest release rate since the presence of macropores significantly decreased the total resistance of the membrane.

When P/S ratio is increased from 5/85 to 10/80 and then to 15/75, macropores disappear as shown in Figure 7.2 and Figure 7.9, respectively. In the membrane prepared from the solution consisting of P/S ratio of 10/80, the total resistance of the membrane is controlled by the resistance of the skin layer as indicated by the ratio of $R_{\text{skin}}/R_{\text{substrate}}=19$. However, when P/S ratio is increased to 15/75, then, both the resistances of the skin layer and the substrate contribute to the overall resistance to transport of drug molecules ($R_{\text{skin}}/R_{\text{substrate}}=52.8/67.2=0.79$). Consequently the release rate significantly decreases as P/S ratio is decreased from 10/80 to 15/75.

The same relationship between the release rate and the P/S ratio was observed when composition of water in the solution was increased to 15%. SEM pictures of the membranes having initial P/S ratio of 5/80, 10/75 and 15/70 are shown in Figures 7.10 through 7.12.

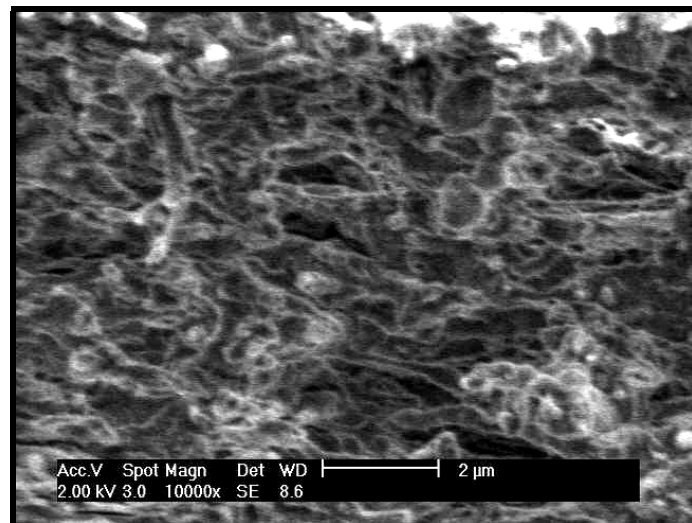


Figure 7.10. SEM picture of cross section of a membrane. Initial composition: 5% CA, 80% Acetone, 15% Water. Magnificationx10000.

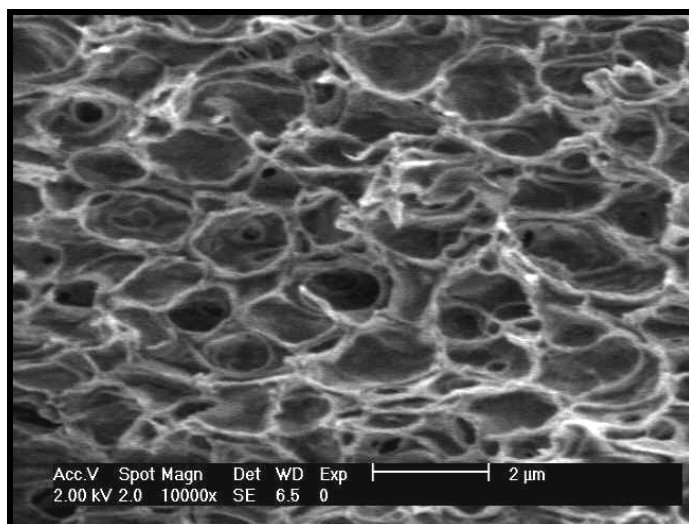


Figure 7.11. SEM picture of cross section of a membrane. Initial composition: 10% CA, 75% Acetone, 15% Water. Magnificationx10000.

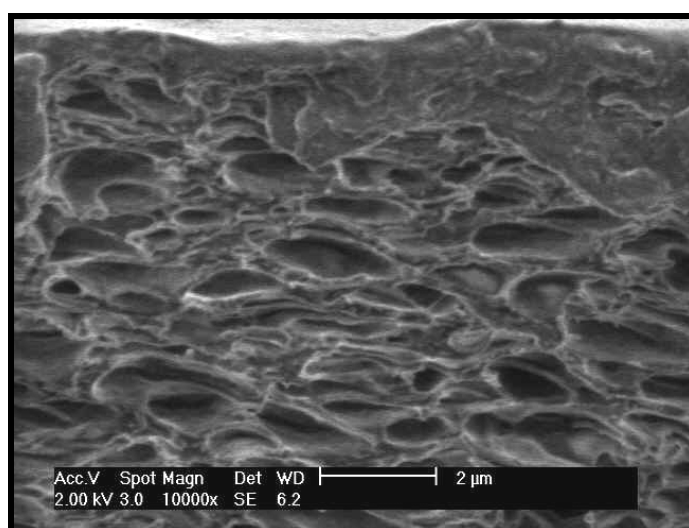


Figure 7.12. SEM picture of cross section of a membrane. Initial composition: 15% CA, 70% Acetone, 15% Water. Magnificationx10000.

The membrane prepared from the lowest polymer concentration of 5%, is very thin compared to the other membranes. From SEM picture shown in Figure 7.10, the overall thickness and the average pore size were determined as 10.52 μm and 0.885 μm , respectively. The overall resistance of this thin membrane is lower than the others, thus, the highest release rate was observed for the lowest P/S ratio of 5/85. When the initial

P/S ratio is increased to 10/75, average pore size increases to 1.16 μm . It was determined from Figure 7.11 that, membrane has uniform sponge type cylindrical pores with a narrow pore size distribution. The membrane prepared from the initial P/S ratio of 15/70 has also sponge like substructure, however, pore size distribution is wider than the membrane having P/S ratio of 10/75, as shown in Figure 7.12. In the membrane prepared from the initial P/S ratio of 10/75, the decrease in release rate as P/S ratio is increased from 10/75 to 15/70 is associated with both the change in pore size distribution from narrow to wide and the increase in both the resistance of the skin layer and the substrate. Consequently, the drug release rate decreases significantly with an increase in overall resistance to passage of drug molecules.

7.1.3. Effect of Polymer / Nonsolvent (P/NS) Ratio on Release Rate

To investigate the effect of P/NS ratio on drug release rate, tablets were coated with solutions consisting of 80 w% acetone and 15/5, 10/10, 5/15 and 3/17 P/NS ratios.

Figure 7.13 shows that release rate exponentially decreases with increasing P/NS ratio.

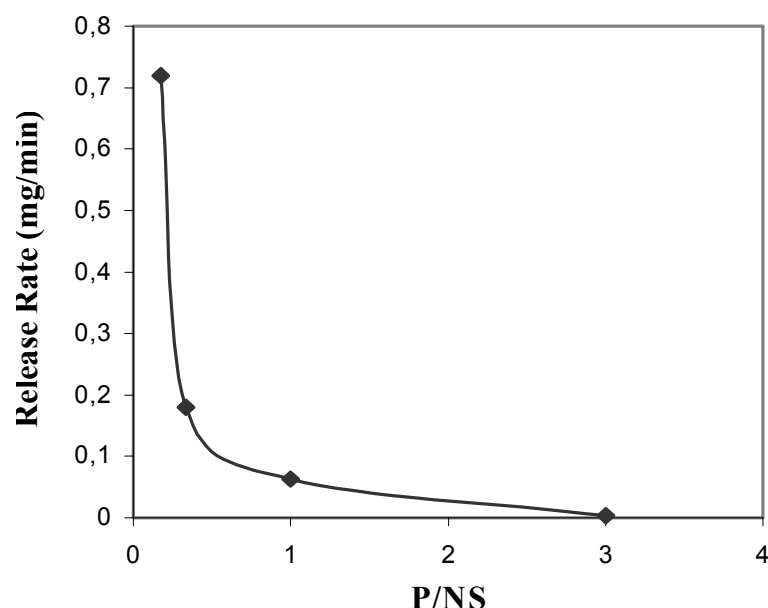


Figure 7.13. Release rate of theophylline as a function of P/NS ratio for 80% acetone content.

SEM picture of the membrane prepared from the lowest polymer composition, 3% CA, is shown in Figure 7.14.

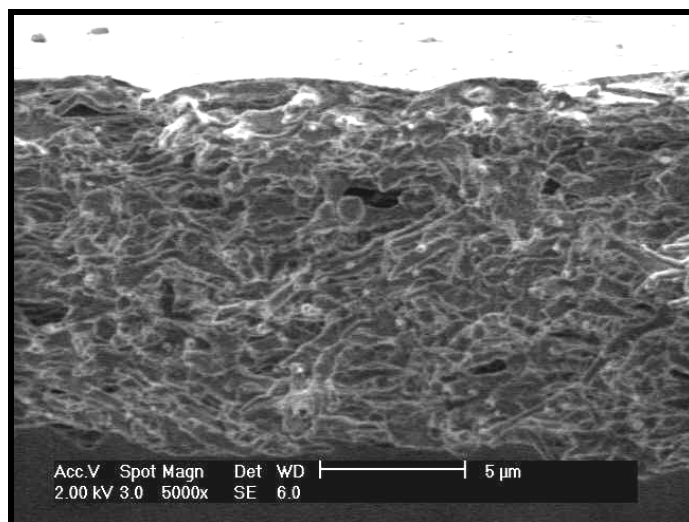


Figure 7.14. SEM picture of cross section of a membrane. Initial composition: 3% CA, 80% Acetone, 17% Water. Magnificationx5000.

This membrane has the highest drug release rate since it has almost no dense skin layer and thus its porosity is higher than the others. It has a porous structure with irregular pore shapes. The decrease in release rate with increase in P/NS ratio from 0.18 to 3 is associated with the decrease in porosity of the membrane from 34% to 16.5%. The change in morphology of the membranes with increasing P/NS ratio can be seen in Figures 7.14, 7.10, 7.2, 7.5, respectively. The increase in P/NS ratio also leads to an increase in contribution of the resistance of the substrate layer. The fraction of the skin layer resistance ($R_{\text{skin}}/R_{\text{total}}$) decreases from 0.95 to 0.23 as P/NS ratio is increased from 1 to 3. This is an expected result, since with a decrease in porosity of the membrane, amount of polymer and its corresponding resistance in the substructure increases leading to increase in contribution of the substrate resistance.

7.1.4. Effect of Solvent / Nonsolvent (S/NS) Ratio on Release Rate

The effect of solvent-nonsolvent ratio was investigated by coating the tablets with polymer solutions consisting of 10% cellulose acetate and 85/5, 75/15 and 80/10 and finally 15% cellulose acetate and 80/5, 70/15, and 75/10. Figure 7.15 shows the effect of S/NS ratio on the release rate with different polymer contents.

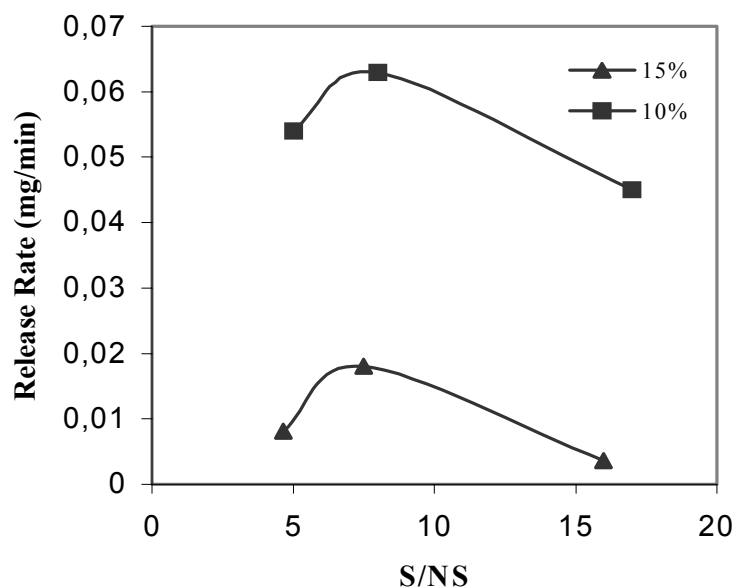


Figure 7.15. Release rate of theophylline as a function of S/NS ratio for 10% and 15% polymer content.

According to Figure 7.15 a maximum in release rate was observed with increasing S/NS ratio. When polymer composition is 10%, an increase in release rate was observed by increasing S/NS ratio from 75/15 to 80/10 due to a decrease in contribution of substrate resistance. The ratio of resistance of the skin layer to that of the substrate, $R_{\text{skin}}/R_{\text{substrate}}$, increases from 0.77 to 19 as S/NS is varied from 75/15 to 80/10. Hence, in the membrane, prepared from 10% CA, 80% acetone, 10% water, total resistance is very small which occurs only 7% of the overall thickness. As a result, this membrane shows the maximum release rate. Further increase in S/NS ratio from 80/10 to 85/5 leads to a change in morphology from more porous to a dense one as shown in Figure 7.2 and 7.6, respectively.

Similarly, when polymer composition is 15%, release rate increases and reaches to the maximum as S/NS ratio was increased from 70/15 to 75/10 and then starts to decrease as S/NS ratio was increased further to 80/5. This is due to changes in effect of individual resistances on the overall resistance. At low S/NS ratios, the resistance of the skin layer becomes more dominant, thus, with increasing S/NS ratios the release rate increases. However, at high S/NS ratios, the resistance of the substrate layer increases with increasing S/NS ratios leading to decrease in the release rates. Consequently, the

balance between the resistance of the skin layer and the resistance of the sublayer causes an observation of the maximum in the release rates.

7.1.5. Effect of Number of Coatings on Release Rate

The effect of number of coatings on release rate was investigated by coating the tablets 1, 2 and 3 times with the solution consisting of 10 w% cellulose acetate, 80 w% acetone and 10 w% water. Dipping time for each coating was 60 sec. Results of the effect of number of coatings on the release rate are shown in Figure 7.16.

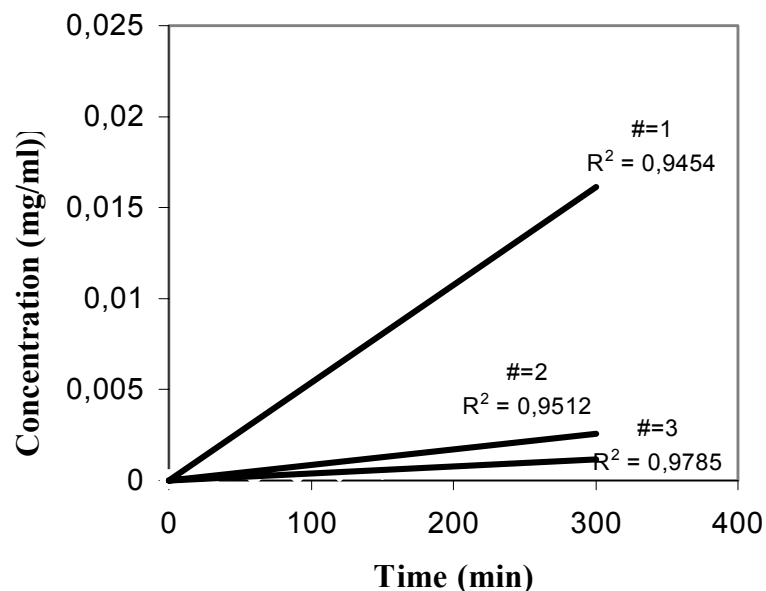


Figure 7.16. Release of theophylline from tablets coated with asymmetric membrane 1, 2 and 3 times.

The decrease in release rate with increasing number of coating is an expected result since resistance to transport of drug and water molecules increases with increasing the length of diffusion path. The rate of drug release from a tablet coated once is almost 15 times higher than the tablet coated 3 times.

7.1.6. Effect of Coating Time on Release Rate

The effect of coating time on release rate was investigated by coating the tablets with two different dipping times, which are 1 and 2 min with the solution consisting of 10 w% cellulose acetate, 80 w% acetone and 10 w% water. The release profiles are shown in Figure 7.17.

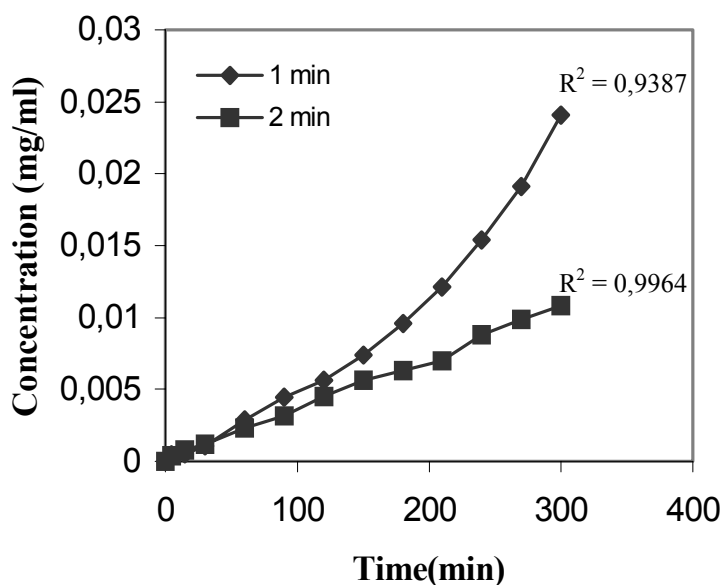


Figure 7.17. Release of theophylline from tablets coated with asymmetric membrane with coating times 1 and 2 min.

The rates of drug release from a tablet coated for 1 and 2 min were calculated as 0.063 and 0.036 mg/min, respectively. The decrease in release rate with increasing the coating time is due to an increase in the amount of coating solution on the tablet that leads to increase in the total thickness and the skin thickness.

7.1.7. Effect of Evaporation Conditions on Release Rate

To investigate the effect of evaporation on the release rate, tablets were coated with 10% CA, 80% acetone and 10% water and then dried under free and forced convection conditions. The release profiles of both types of coated tablets are shown in Figure 7.18.

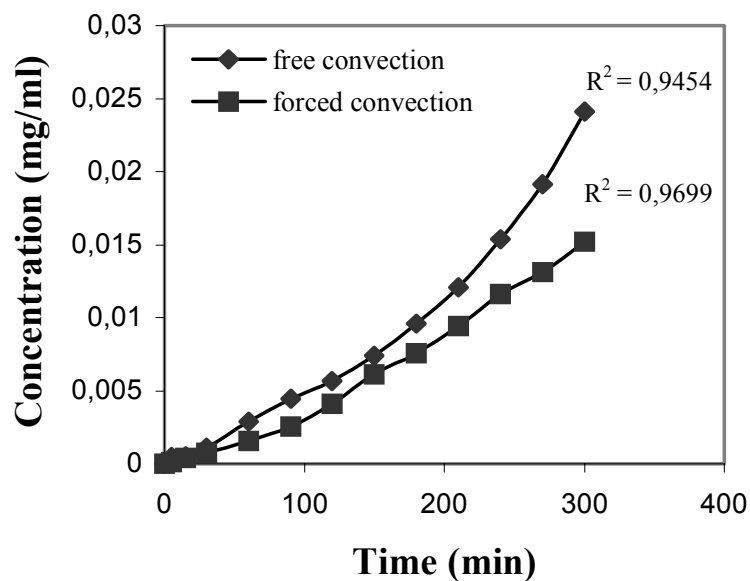


Figure 7.18. Release of theophylline from tablets in which the solvent is evaporated under free and forced convection condition.

The membrane prepared under forced convection condition was transparent indicated that phase separation could not be achieved. This hypothesis was supported by the SEM picture of the membrane shown in Figure 7.19.

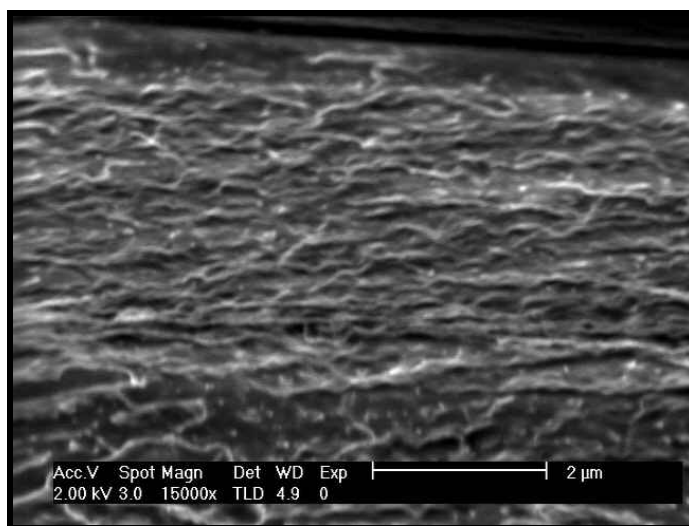


Figure 7.19. SEM picture of cross section of a membrane. Initial composition: 10% CA, 80% Acetone, 10% Water under forced convection condition. Magnificationx15000.

The membrane is completely dense and no porous region is observed while the membrane cast from the same initial composition but dried under free convection conditions has a porous asymmetric structure with 7.1% skin layer as shown previously in Figure 7.2. The change in structure from porous/asymmetric to a dense one leads to a drop in release rate from 0.063 mg/min to 0.045 mg/min.

The membrane formation process is very complex influenced by both thermodynamic and kinetic factors. When the speed of air in the drying atmosphere is increased, the rate of evaporation of solvent increases dramatically and within a short time, its concentration at the free surface of the membrane solution drops to zero. This leads to very strong diffusional resistance within the membrane and slow evaporation of the nonsolvent. Consequently two phase region boundary is never reached and the resulting membrane structure becomes dense due to the lack of phase separation.

The results shown in Figure 7.18 suggest that evaporation step during membrane preparation has a significant effect on the resulting membrane structure. Simply, by varying the evaporation condition, membranes with totally different structures can be produced from the same polymer/solvent/nonsolvent combination.

7.1.8. Effect of Types of Nonsolvent on Release Rate

To investigate the effect of nonsolvent type on the release rate, tablets were coated with solutions consisted of 10% CA, 80% Ac and 10% nonsolvent which were water, formamide, 1-octanol, glycerol and 1-hexanol. The effect of nonsolvent type on the release rate of theophylline is illustrated in Figure 7.20. To examine the morphology of the membranes and its effect on the release rate, SEM pictures were taken as shown in Figures 7.21 through 7.27. The phase analysis was conducted on each membrane and the results are listed in Table 7.3.

Table 7.3. The release rate and the results of phase analysis of the membranes prepared from different nonsolvents.

Nonsolvent	Release Rate (mg/min)	R ²	Porosity (%)	L _{total} (μm)	L _{skin} (μm)	Average Pore Size (μm)	Skin %
Octanol	0.360	0.9590	17.01	32.92	1.57	0.50	4.7
Water	0.063	0.9454	22.33	16.05	1.14	1.04	7.1
Formamide	0.036	0.9812	Dense	12.84	1.60	0.53	12.4
Glycerol	0.036	0.9830	37.73	39.56	4.83	16.78	12.2
Hexanol	0.027	0.9604	44.00	24.90	3.35	1.24	13.4

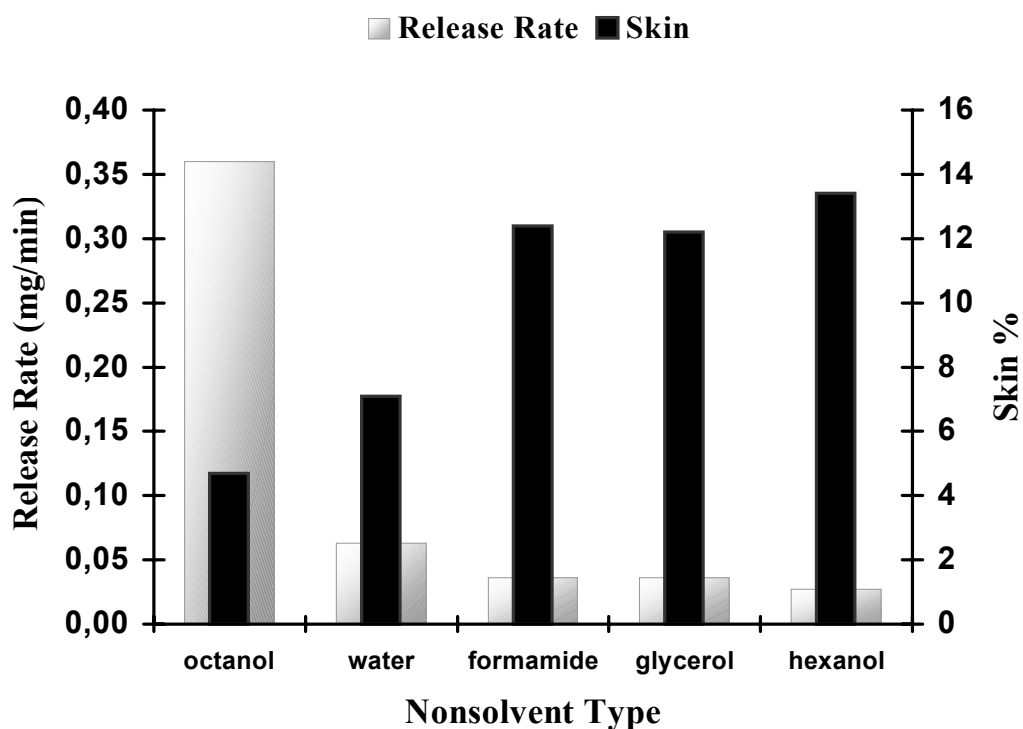


Figure 7.20. The release of theophylline from tablet coatings prepared from CA/Acetone and different nonsolvents and the skin percents of these membranes.

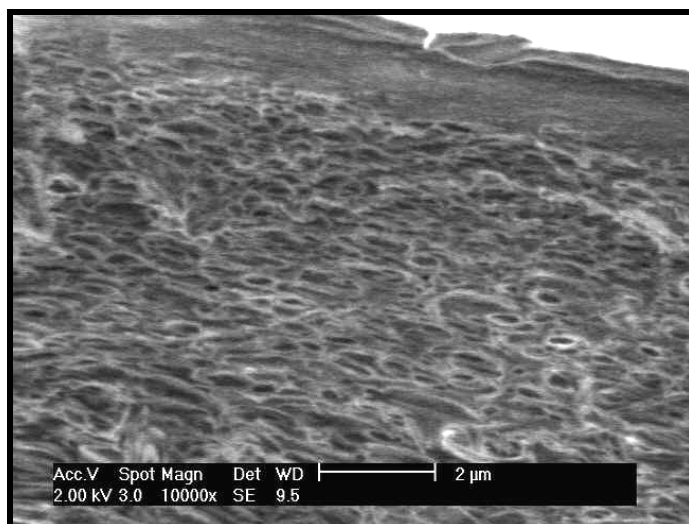


Figure 7.21. SEM picture of cross section of a membrane. Initial composition: 10% CA, 80% Acetone, 10% Octanol. Magnificationx10000.

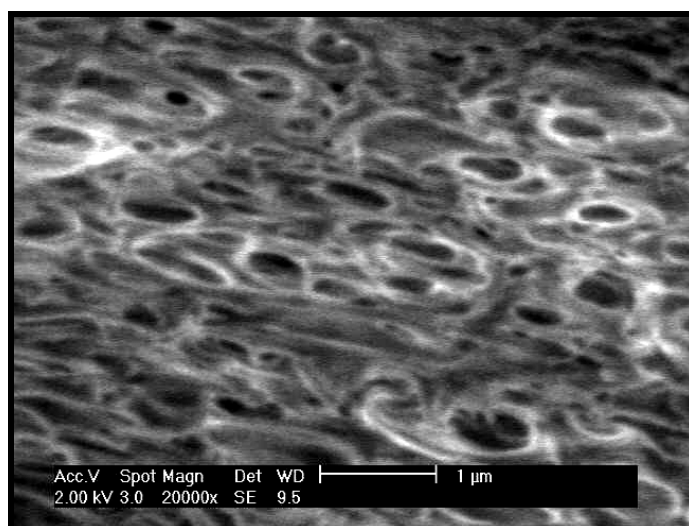


Figure 7.22. SEM picture of cross section of a membrane. Initial composition: 10% CA, 80% Acetone, 10% Octanol. Magnificationx20000.

The membrane prepared using 1-octanol as nonsolvent has small pores having average pore size of 0.5 μm. The pores have uniform cylindrical shapes, which can be easily observed in Figure 7.22 with the magnification of 20000. This membrane has the highest release rate since it has the smallest percentage of skin layer among the other membranes.

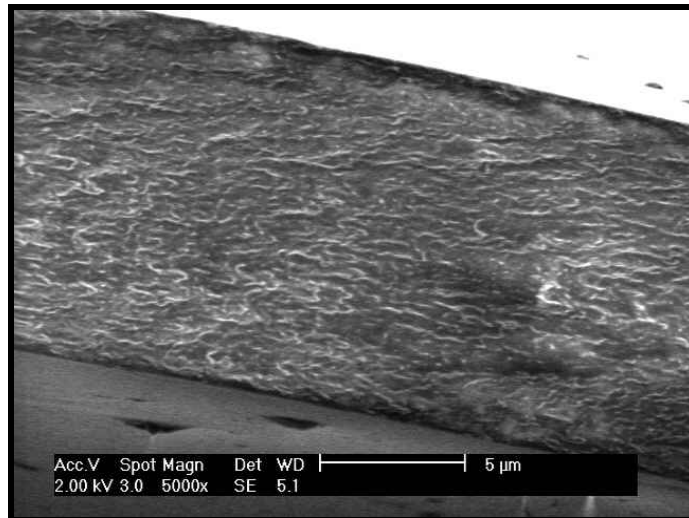


Figure 7.23. SEM picture of cross section of a membrane. Initial composition: 10% CA, 80% Acetone, 10% Formamide. Magnificationx5000.

Membrane prepared from formamide were transparent indicated that no phase separation occurred. The resulting structure is dense and shown in Figure 7.23.

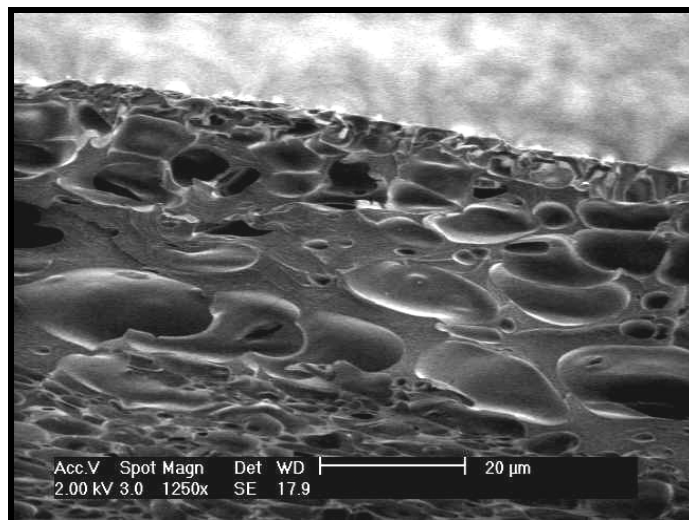


Figure 7.24. SEM picture of cross section of a membrane. Initial composition: 10% CA, 80% Acetone, 10% Glycerol. Magnificationx1250.

Macrovoids were observed in membrane prepared from glycerol as shown in Figure 7.24. Due to the presence of macrovoids, the overall thickness of the membrane is highest among the others.

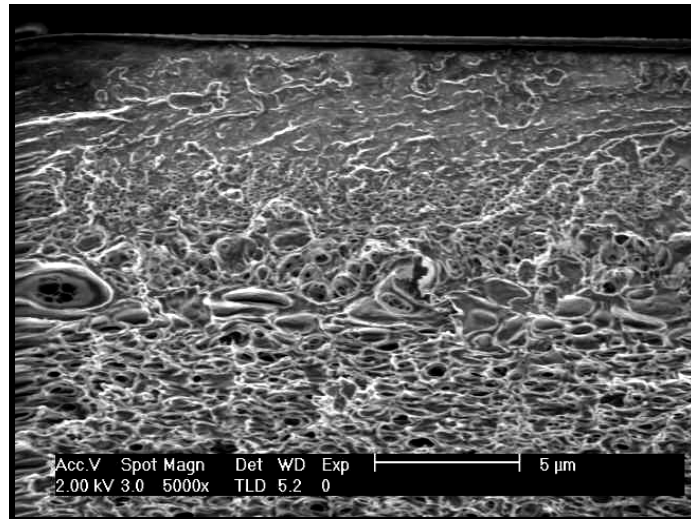


Figure 7.25. SEM picture of cross section of a membrane. Initial composition: 10% CA, 80% Acetone, 10% Hexanol. Magnificationx5000.

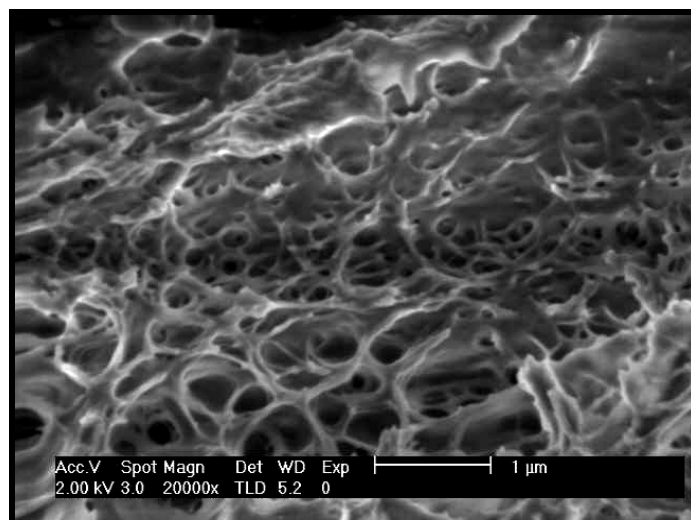


Figure 7.26. SEM picture of the top layer of membrane. Initial composition: 10% CA, 80% Acetone, 10% Hexanol. Magnificationx20000.

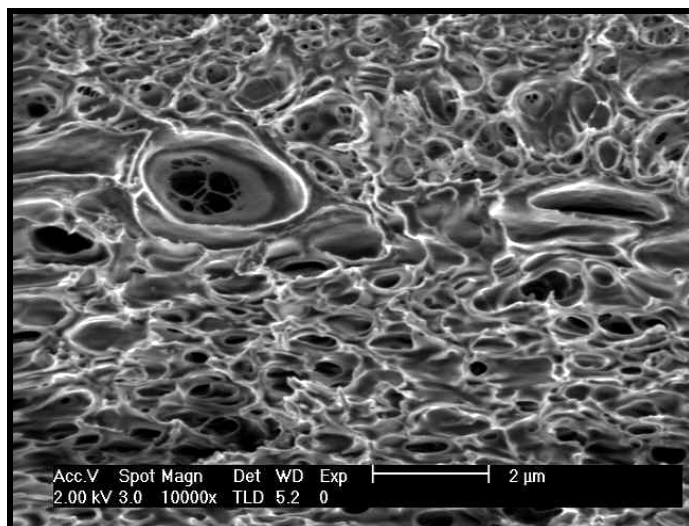


Figure 7.27. SEM picture of the mid section of membrane. Initial composition: 10% CA, 80% Acetone, 10% Hexanol. Magnificationx10000.

The membrane prepared from 1-hexanol has uniform cylindrical pores with the average size of 1.24 μm and 13.4% skin layer that is the maximum value compared to the other membranes. Figure 7.25 through 7.27 show SEM pictures of the cross section, top and the mid of the cross section of this membrane. At the top of the membrane, there is sponge like structure and pores are interconnected to each other while in the middle section macropores were observed, thus, the membrane has a large pore size distribution.

The change in % of skin layer with the nonsolvent type is also plotted in Figure 7.20. According to this figure, the decrease in release rate is associated with the increase in the resistance of the skin layer.

Diversity in the morphologies of the membranes prepared from different nonsolvents is due to complex mechanism of membrane formation. The membrane formation process and subsequent structure is not only influenced by initial composition and preparation conditions but it is also affected by the thermodynamic behavior and the diffusional characteristics of the components in the membrane solution.

7.2. Permeability Studies

Membranes cast from solutions of cellulose acetate (CA), acetone (Ac), water (W) were used to investigate the permeability characteristics. Initial casting thickness of the membranes was 300 μm . Six different types of asymmetric membranes were prepared by varying the composition. To illustrate the advantage of the asymmetric membranes, permeability of dense membrane prepared from the solution of cellulose acetate dissolved in acetone was also measured.

Permeabilities were determined using the diaphragm cell model discussed in Chapter 4 in section 4.3. For this purpose, equations 4.17 and 4.18 were applied to fit the experimental data consisting of the concentrations in the donor and receiver compartments at different times. In these equations, the permeability, P_{eff} , was used as a fitting parameter. The nonlinear curve fitting was performed using solver tool in Excel by minimizing the sum of the squared errors:

$$\sum_{i=1}^N \left(\frac{c_D^{\text{exp}} - c_D^{\text{model}}}{c_D^{\text{exp}}} \right)^2 + \sum_{i=1}^N \left(\frac{c_R^{\text{exp}} - c_R^{\text{model}}}{c_R^{\text{model}}} \right)^2 \rightarrow 0 \quad (7.4)$$

Table 7.4. lists the values of permeabilities determined from the nonlinear regression analysis.

Table 7.4. Permeability and thickness of the membranes.

Composition			Permeability (cm^2/min)	Total Thickness (μm)	Skin Thickness (μm)
CA	Ac	W			
10	90	0	7.1316×10^{-7}	8.40	-
10	80	10	5.3190×10^{-6}	16.05	1.14
5	80	15	5.7208×10^{-6}	10.52	0.63
15	80	5	2.1149×10^{-6}	15.27	5
5	85	10	1.5913×10^{-5}	26.09	-
15	75	10	7.0210×10^{-6}	20.06	1.85
15	70	15	1.2201×10^{-5}	34.91	2.58

Figure 7.28 shows the variation of reduced permeability with the percentage of the skin layer.

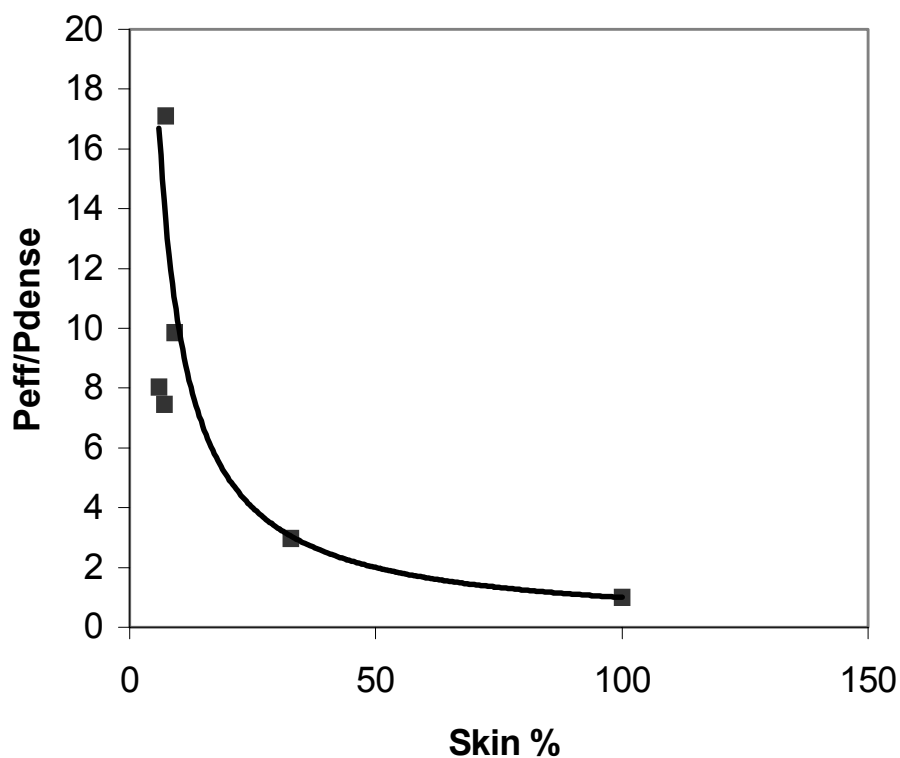


Figure 7.28. Relationship between the percentage of skin layer and P_{eff} / P_{dense} ratio.

Reduced permeabilities were calculated by dividing the permeability of asymmetric membrane to that of the dense membrane. According to the results shown in Figure 7.28, normalized permeability of the asymmetric membranes decreases exponentially with the increase in the percentage of the skin layer. Thus, the increase in thickness of the skin layer leads to the increase in overall resistance to transport of drug molecules and consequently the decrease in permeabilities.

The results shown in Figure 7.28 point out that the permeability of the asymmetric type coating can be adjusted by controlling the membrane structure. Thus, release kinetics of drug can be controlled without changing the coating material or significantly varying the overall coating thickness.

7.3. Statistical Analysis of Experiments

7.3.1. Determination of the Variables and Feasible Region for the Design of Experiments

As a first step in designing the experiments, the variables influencing the response chosen as the release rate of the theophylline were determined. These are initial composition of the coating solution, type of nonsolvent, number of coatings, coating time and evaporation condition. Based on the preliminary results of the experiments and the literature data, it was concluded that the most influential parameter on the membrane structure and thus on the release rate is the initial composition of the coating solution. Consequently, the experiments were designed to find relationship of

$$\text{The release rate} = f(x_1, x_2, x_3)$$

in which x_1 , x_2 , x_3 are the compositions of the cellulose acetate, acetone and water in weight percentages, respectively. The second step in the design of experiments was to determine the range of variables, i.e, the design region. The composition of each component has both upper and lower bound constraints which were determined based on the simulation results of Özbaş (2001) and the available literature data. These constraints are:

$$\begin{aligned} 5 &\leq x_1 \leq 15 \\ 70 &\leq x_2 \leq 90 \\ 5 &\leq x_3 \leq 15 \end{aligned}$$

Figure 7.29 shows the feasible region for the design of experiments in a ternary diagram.

7.3.2. Mixture Design

The experimental region shown in Figure 7.29 is not a standard shape, i.e., the feasible region is not a simplex. Therefore, the D-optimal design was generated using commercial software called Design-Expert. The results of the design are listed in Table 7.5 and the constrained experimental region with the experimental run points is shown in Figure 7.30.

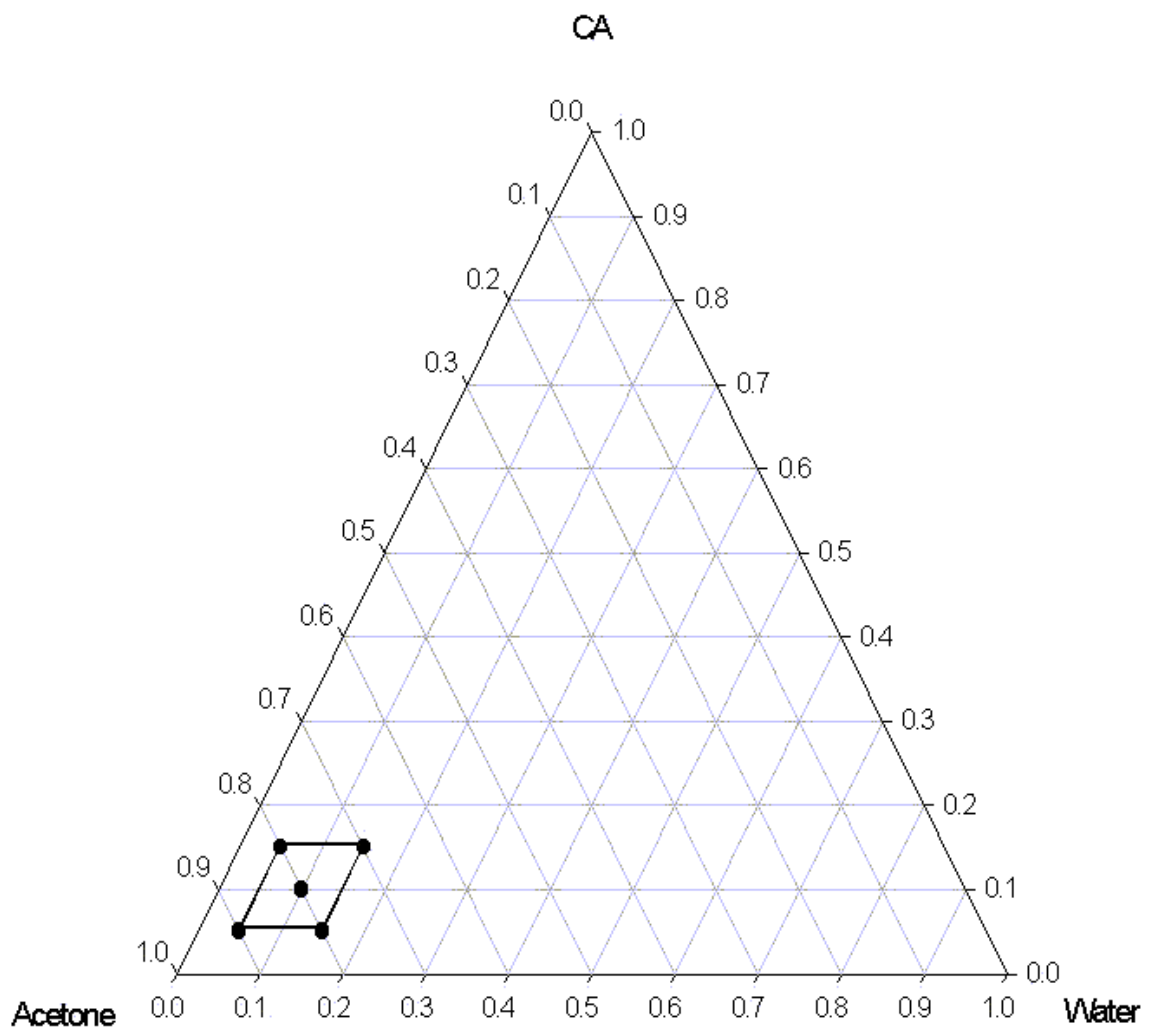


Figure 7.29. The feasible region for the design of experiments

Table 7.5. D-optimal design for the mixture of membrane solution.

Standard Order	A: Cellulose Acetate	B: Acetone	C: Water
1	15	80	5
2	15	80	5
3	5	90	5
4	5	90	5
5	15	70	15
6	15	70	15
7	5	80	15
8	5	80	15
9	5	85	10
10	10	80	10
11	15	75	10
12	10	85	5
13	77.5	12.5	10
14	10	75	15

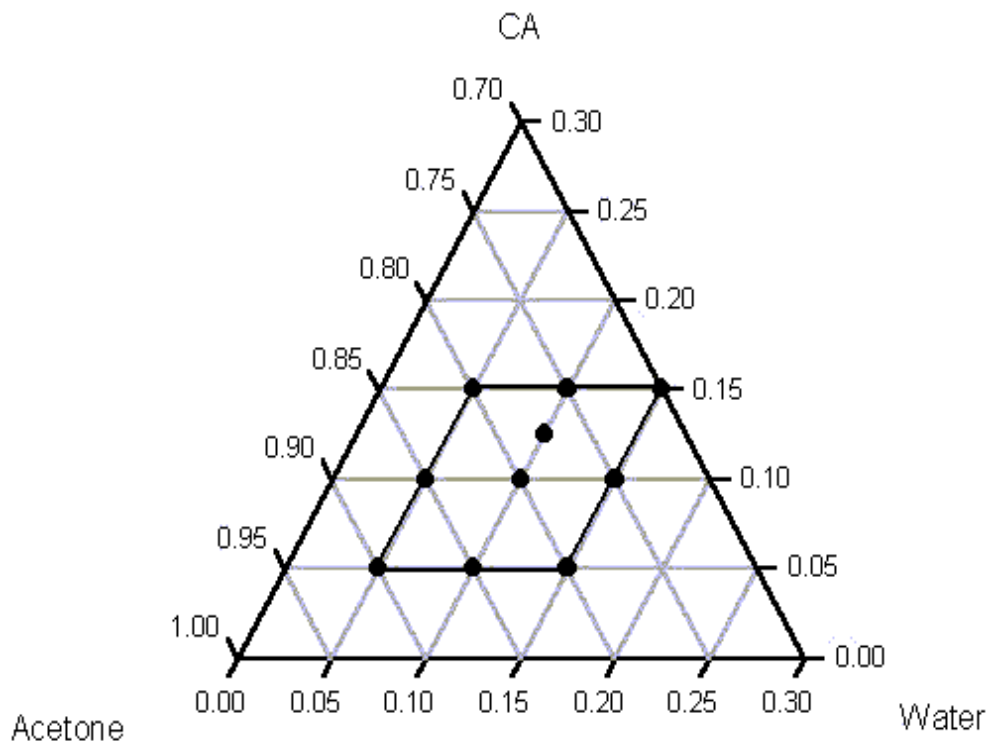


Figure 7.30. The constrained experimental region the design of experiments.

In the 14-run design, six experimental runs are required to fit the quadratic mixture model, four additional distinct runs are required to check for the lack of fit and finally four runs are replicated to provide an estimate of pure error. According to the results shown in Table 7.5, Design-Expert used the vertices, the edge centers, the overall centroid and one point located halfway between the overall centroid and one of the edge centers as candidate points. Additionally, four vertices of the design region were used again as check points.

7.3.3. The Regression Model and Statistical Analysis

The statistical analysis of the experimental results was performed using Design-Expert software package. The output from this program is shown in Appendix C. The data was best fitted to the special cubic equation. The resulting equation for predicting the release rate of theophylline is given as follows:

$$\begin{aligned} \text{The Release Rate} = & 40.38107 x_1 + 1.27250 x_2 + 26.64414 x_3 - 56.47210 x_1 x_2 \\ & -260.60344 x_1 x_3 - 37.10052 x_2 x_3 + 301.559710 x_1 x_2 x_3 \end{aligned} \quad (7.5)$$

The statistical analyses of the experimental release rate data are given in Tables 7.6 and 7.7. In Table 7.6, an analysis of variance (ANOVA) for the model given in equation 7.5 is presented. The first line of the analysis of variance is an overall summary for the full model. The symbols A, B, C refer to cellulose acetate, acetone and water, respectively. The sum of squares is used as a measure of overall variability in the data. The value of 0.17 indicates that variation in the experimental data is very small. Mean square values are obtained by dividing the sum of squares by the degrees of freedom. The model F-value of 39.97 implies that the model is significant. There is only a 0.01% chance that a “Model F-value” this large occurs due to noise. The importance of each term, i.e., the influence of cross interaction between/among the components on the release rate is shown by the values in column “Prob>F”. Values of “Prob>F” less than 0.05 indicate that model terms are significant. In this case, the interaction between cellulose acetate (A) and acetone (B) has the largest influence on the release rate of theophylline since the value of Prob>F is the smallest for the model term AB. The interaction between acetone and water has the least influence on the release rate of theophylline. Values of “Prob>F” greater than 0.1 indicate that the model terms are not significant.

Table 7.6. Analysis of Variance (ANOVA) for the release rate data.

Source	Sum of Squares	DF	Mean Square	F Value	Prob>F	
Model	0.17	6	0.028	39.97	<0.0001	significant
Linear Mixture	0.14	2	0.069	98.25	<0.0001	
AB	0.014	1	0.014	20.29	0.0028	
AC	7.212E-3	1	7.212E-3	10.30	0.0149	
BC	4.123E-3	1	4.123E-3	5.89	0.0457	
ABC	4.779E-3	1	4.779E-3	6.82	0.0348	
Residual	4.902E-3	7	7.003E-4			not significant
Lack of Fit	8.518E-4	3	2.839E-4	0.28	0.8378	
Pure Error	4.050E-3	4	1.013E-3			
Cor Total	0.17	13				

Table 7.7. Statistical analysis of the release rate data.

Std. Dev.	0.026
Mean	0.099
C.V	26.82
PRESS	0.020
R ²	0.9716
Adj. R ²	0.9473
Pred. R ²	0.8851
Adeq. Precision	16.631

Table 7.7 lists the results of several R² statistics. Simply, the ordinary R² measures the proportion of total variability explained by the analysis of variance model. The large value of R², close to 1 is desirable. There are some other R² statistics displayed in the table. The adjusted R² reflects the number of factors in the model. “Std.Dev.” is the square root of the error mean square. “C.V.” is the coefficient of variation which measures the unexplained or residual variability in the data. “PRESS” stands for “Prediction Error Sum of Squares” and it is a measure of how well the regression model is likely to predict the response in a new experiment. Small values of PRESS are desirable, since it indicates that the model is likely to be a good predictor. The “Adequate Precision” is computed by dividing the difference between the maximum and minimum predicted release rates by the average standard deviation of all predicted release rates. Large values of this quantity are desirable, the value of 16.6 in Table 7.7

points out that the model given in equation 7.5 will give reasonable performance in prediction. The “Lack of Fit F-Value” of 0.28 implies the Lack of Fit is not significant relative to the pure error. Non-significant lack of fit is an indication of the accuracy of the model used to fit the experimental data.

7.3.4. The Response Surface Plot

Figure 7.31 presents contour plots of the surface generated by the model equation shown in equation 7.5.

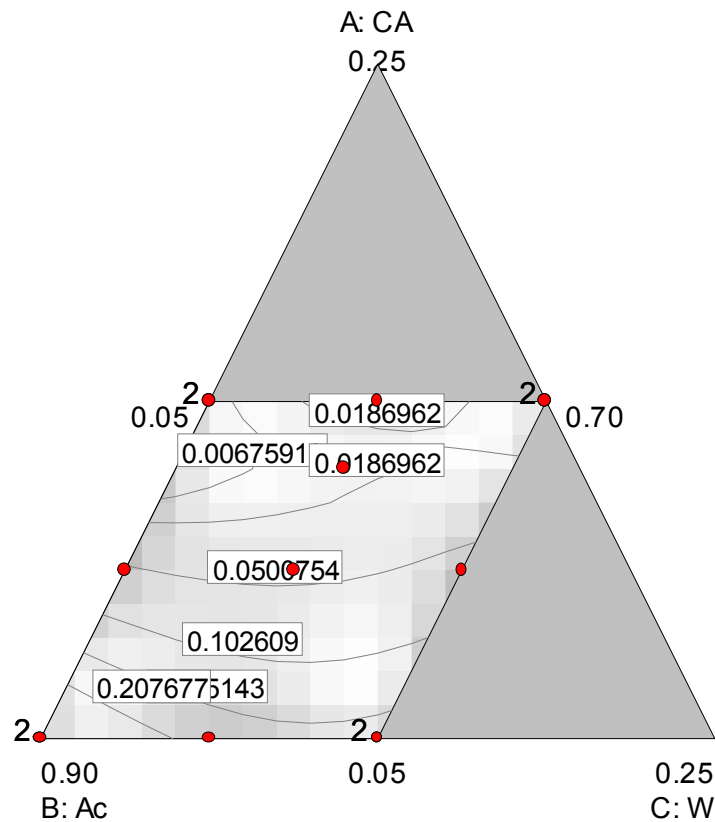
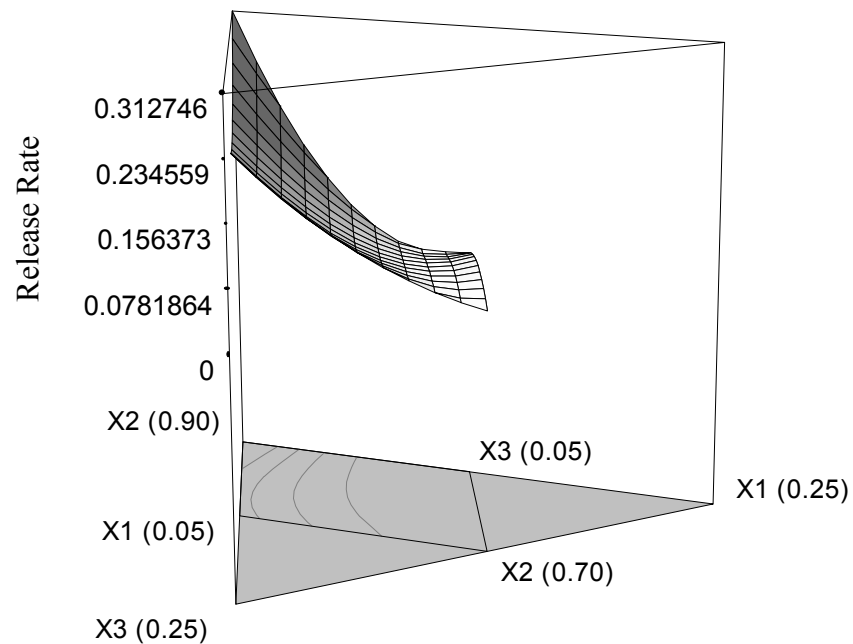
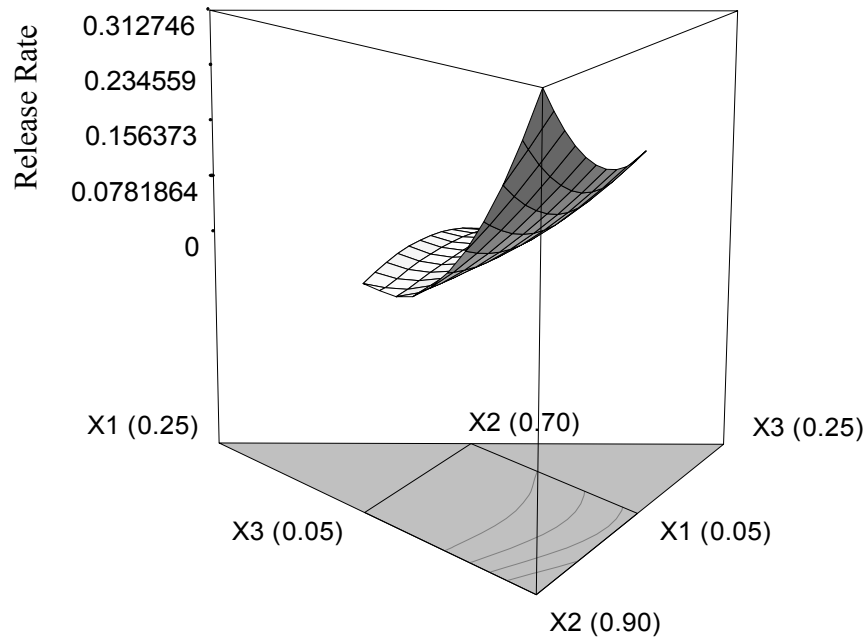


Figure 7.31. Contour plots in the D-optimal design area.

The feasible region is shown by the unshaded region. The circles represent the design points while number 2 at corners indicates the repeated experimental points. Contour plots are useful since they can provide compositions that can be chosen for a given release rate of theophylline. The three dimensional surface plots shown in Figure 7.32

provide essentially the same information. These three successive plots show the response surfaces from different perspectives. The results shown in Figure 7.32 indicate that within the experimental region, the maximum release rate of theophylline is 0.312 mg/min which is obtained when the compositions of cellulose acetate, acetone and water are 5%, 90% and 5% respectively.



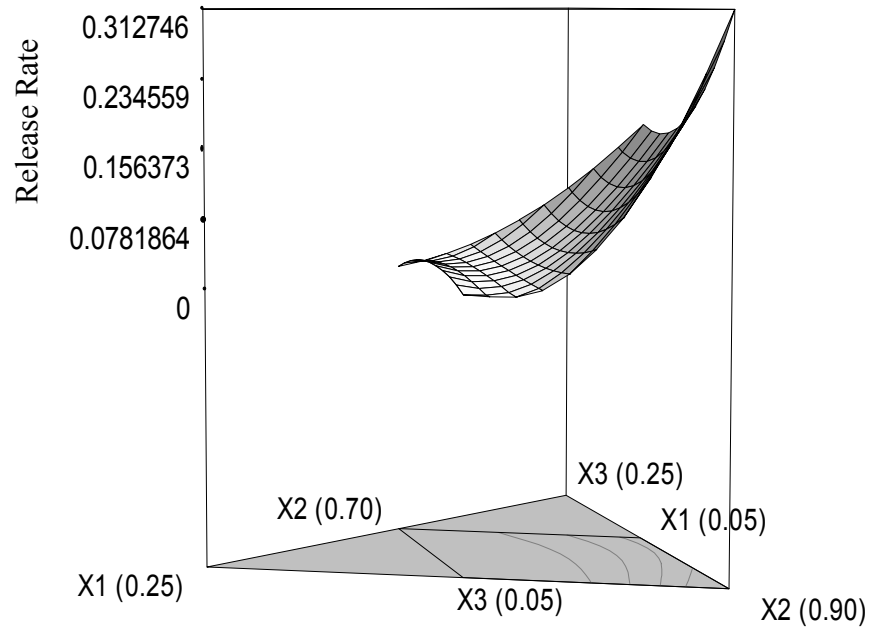


Figure.7.32. Three dimensional surface plot for design area.

CONCLUSION

In this study, asymmetric type of coatings have been applied to tablets. The advantages of these type of coatings over the conventional dense coatings were demonstrated both by dissolution and permeability studies. The advantages are acquired due to flexibility in changing the structure of the coating by varying the preparation conditions. In particular, the effects of composition of the membrane solution, the type of nonsolvent, coating time, number of coating layers and evaporation conditions on the release rate and the structure of the membrane were examined. In these experiments, one factor-at-a-time approach was followed in which only factor being investigated was varied while all other factors were held constant at the baseline set of levels. The baseline levels of variables were chosen as follows: Initial composition: 10 w% polymer (cellulose acetate), 80 w% solvent (acetone) and 10 w% nonsolvent (water), coating time: 1 min, number of coating layer: 1, evaporation condition: free convection. According to this baseline scheme, the increase in coating time and the number of coating layers decreased the release rate of theophylline. The decrease in each case is due to the increase in transport resistance to drug molecules associated with an increase in length of the diffusion path. Evaporation condition was found to have a significant influence on the structure and thus the release rate of the drug. The change in evaporation condition during drying of coated tablets from free convection to forced convection caused a substantial decrease in release rate of drug. The scanning electron microscope pictures of both membranes indicated that the structure changed from asymmetric porous type to a dense one as air was blown harder to dry tablets. In addition to water, octanol, hexanol, glycerol and formamide were used as nonsolvents in the coating solution. The highest release rate was obtained with octanol, while, the coating prepared from hexanol gave the lowest release rate of drug. The comparison of scanning electron microscope pictures of the membranes pointed out that the decrease in release rate of the membranes prepared from different nonsolvents was due to the increase in the thickness of the dense skin layer, thus, the increase in resistance of this layer. Statistical design of experiments was performed to draw more meaningful and objective conclusions from the data. In the design of experiments, the compositions of cellulose acetate, acetone and water were chosen as the parameters influencing the release rate of the drug. The results of the statistically designed experiments have shown that the

increase in P/NS ratio caused an exponential decrease in release rate. From the detailed phase analysis and structure of the membranes, it was seen that the increase in P/NS ratio leads to a decrease in porosity of the membranes, while the fraction of dense skin layer increased. Thus both the resistance of the skin layer as well as the resistance of the substrate increased. However, the contribution of substrate resistance on the overall resistance was found to be more dominant with increasing P/NS ratio. The same trend was observed with increasing P/S ratio. In particular, the effect of substrate resistance becomes more important as P/S ratio increases leading to increase in overall resistance to transport of drug, and thus, substantial decrease in release rate. At higher polymer concentrations, a maximum in release rate was observed as S/NS ratio was increased. At low S/NS ratios, the resistance of skin layer becomes more important while at high S/NS ratios, the contribution of the substrate resistance is larger. The results of statistically designed experiments indicated that the release rate of theophylline can be considerably changed by varying P/S, P/NS or S/NS ratios without changing the coating material or solvent, nonsolvent type. In addition, the statistical analysis of the experimental data and the regression model pointed out that the interactions between cellulose acetate/acetone have the most prominent effect on the release rate of theophylline. However, the interactions between cellulose acetate/water and acetone/water also influence the release rate of theophylline. Permeability studies also indicated that the permeability of the coating to drug molecules can be adjusted by varying the composition of the membrane solution. The advantage of the asymmetric type coating on tablets is not only adjusting the release rate of drug by varying the preparation conditions. All of the results from dissolution studies indicated the fulfillment of the zero-order release requirement for controlled-release systems. It can be finally concluded that asymmetric membrane tablet coatings could provide improved drug delivery formulations capable of releasing the drug at constant and desired rates.

Future work should involve the investigation of solvent type, combination of solvents and nonsolvents in the coating solution as well as the composite coatings prepared from different polymers.

REFERENCES

1. Ansel H.C, Popovivch N.G., Pharmaceutical Dosage Forms and Drug Delivery Systems, (Lea and Febiger, 1990).
2. Bell C.L., Peppas .A.,”Measurement of the swelling force in ionic polymer networks. III. Swelling force of interpolymer complexes,” *Journal of Controlled Release*, 37, (1995), 277.
3. Bettini R., Colombo P., Peppas N.A., “Solubility effects of drug transport through pH-sensitive, swelling-controlled release systems: Transport of theophylline and metoclopramide monohydrochloride,” *Journal of Controlled Release*, 37, (1995).
4. Cahn R.W., Haasen P., “ Medical and Dental Materials” in Materials Science and Technology, vol.14, (1992).
5. Colombo P., Bettini R., Ascentiis A.D. , Peppas N.A., “Analysis of the swelling and release mechanisms from drug delivery systems with emphasis on drug solubility and water transport,” *Journal of Controlled Release*, 39, (1996), 231.
6. Cussler E.L., Diffusion, Mass Transfer in Fluid Systems, (Cambridge University Press, 2nd Edition, 1997)
7. Graham P.D., Brodbeck K.J., McHugh A.J., “Phase inversion dynamics of PLGA solutions related to drug delivery,” *Journal of Controlled Release*, 58, (1999), 233.
8. Gren T., Nyström C.,“Porous cellulose matrices containing lipophilic release modifiers- a potential oral extended-release system,” *International Journal of Pharmaceutics*, 184, (1999), 7.
9. Henis J. M.S., Tripodi M.K., “Composite hollow fiber membranes for gas separation: The resistance model approach,” *Journal of Membrane Science*, 8, (1981), 233.

10. Herbig S.M., Cardinal J.R., Korsmeyer R.W., Smith K.L., "Asymmetric-membrane tablet coatings for osmotic drug delivery," *Journal of Controlled Release*, 35, (1995), 127.
11. Huang R.Y.M., "Resistance model approach to asymmetric polyetherimide membranes for pervaporation isopropanol/water mixtures," *Journal of Membrane Science*, 84, (1993), 15-27.
12. Karasulu H.Y., "Jelatin ve diğer değişik polimerlerle hazırlanan matriks tabletler üzerine çalışmalar," Doktora Tezi, Ege Üniversitesi, (1996).
13. Karasulu H.Y., Ertan G., Köse T., Modeling of theophylline release from different geometrical erodible tablets," *European Journal of Pharmaceutics and Biopharmaceutics*", 49, (2000), 177.
14. Langer R.S., Peppas N.A., "Present and future application of biomaterials in controlled drug delivery," *Biomaterials*, 2, (1981), 201.
15. Liu L., Khang G., Rhee J.M., Lee H.B., "Monolithic osmotic tablet system for nifedipine delivery," *Journal of Controlled Release*, 67, (2000b), 309.
16. Liu L., Ku J., Khang G., Lee B., Rhee J.M., Lee H.B., " Nifedipine controlled delivery by sandwiched osmotic tablet system," *Journal of Controlled Release*, 68, (2000a), 145.
17. Montgomery D.C., Design and Analysis of Experiments, (John Wiley & Sons, Inc. 5th Edition, 2001), p.104.
18. Narisawa S., Nagata M., Ito T., Yoshino H., Hirakawa Y., Noda K., "Drug release behavior in gastrointestinal track of beagle dogs from multiple unit type rate-controlled or time-controlled release preparations coated with insoluble polymer-based film," *Journal of Controlled Release*, 33, (1995), 253.
19. Özbaş B., " Modeling of asymmetric membrane formation by dry casting method," M.S. Thesis, İzmir Institute of Technology, (2001).

20. Picker K., Bikane F., "Tablet formation and release from matrix tablets manufactured with cellulose acetate," *International Journal of Pharmaceutics*, 175, (1998), 147.
21. Ristic C., "Ultrasonic Enhancement of Mass Transfer Rates Across Membranes," PhD Thesis, The Pennsylvania State University, (2000).
22. Qiu Y., Chidambaram N., Flood K., "Design and evaluation of layered diffusional matrices for zero-order sustained-release," *Journal of Controlled Release*, 51, (1998), 123.
23. Siepmann J., Peppas N.A., "Hydrophilic matrices for controlled drug delivery: An improved mathematical model to predict the resulting drug release kinetics," *Pharmaceutical Research*, 17, (2000), 1290.
24. Smith K.L., Herbig S.M., "Controlled Release" in *Membrane Handbook* edited by Winston Ho W.S. and Sirkar K.K. (Von Nostrand Reinhold New York, 1992).
25. Streubel A., Siepmann J., Dashevsky, R., Bodmeier R., "pH-independent release of weakly basic drug from water-insoluble and -soluble matrix tablets," *Journal of Controlled Release*, 67, (2000), 101.
26. The United States Pharmacopeia XXIII, (Mack Publishing Co., Easton, 1995).
27. Thombre A.G., Cardinal J.R., DeNoto A.R., Gibbes D.C., "Asymmetric membrane capsules for osmotic drug delivery II. In vitro and in vivo drug release performance," *Journal of Controlled Release*, 57, (1999a).
28. Thombre A.G., Cardinal J.R., DeNoto A.R., Herbig S.M., Smith K.L., "Asymmetric membrane capsules for osmotic drug delivery I. Development of a manufacturing process," *Journal of Controlled Release*, 57, (1999b), 55.
29. Thombre A.G., DeNoto A.R., Gibbes D.C., "Delivery of glipizide from asymmetric membrane capsules using encapsulated excipients," *Journal of Controlled Release*, 60, (1999c), 333.

APPENDIX A

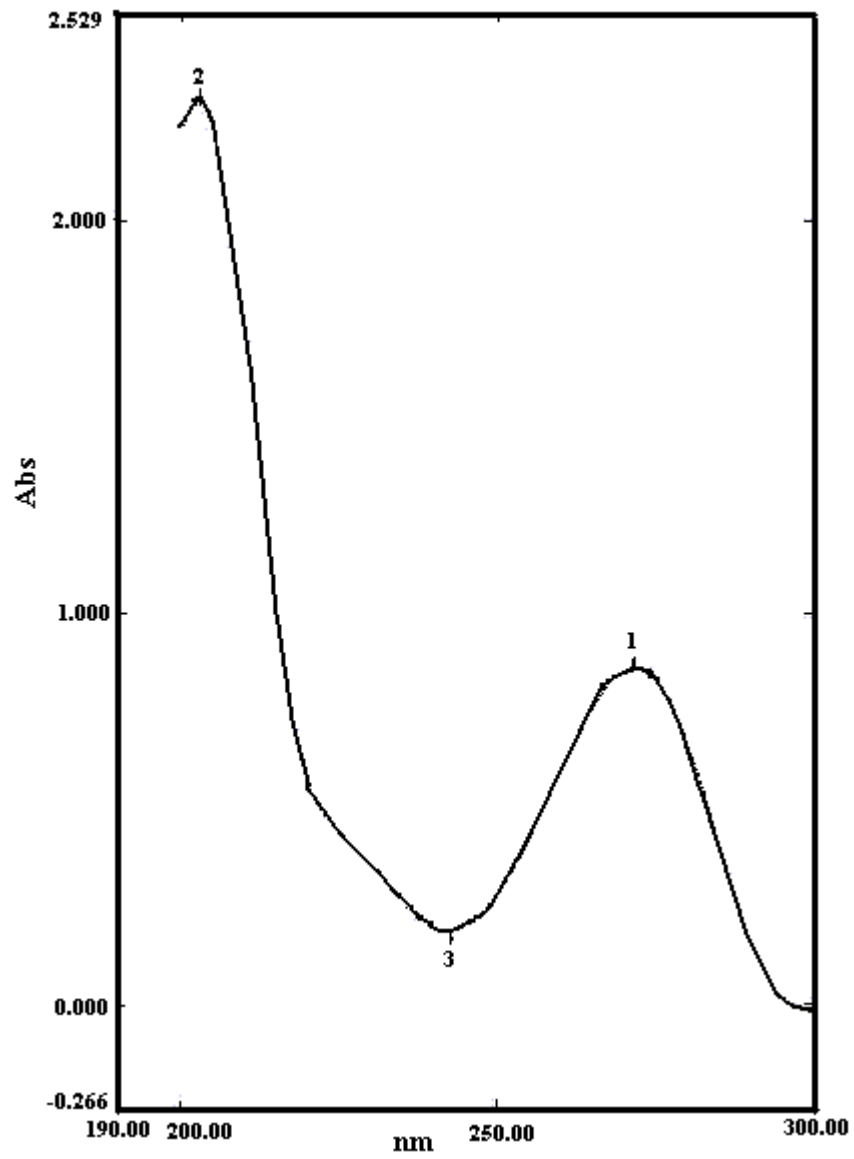


Figure A.1. UV spectrum of theophylline anhydrate in water.

APPENDIX B

Preparation of Solutions For Calibration Curve

0.05 g of theophylline anhydrate was dissolved in 25 ml bidistilled water. From this solution, 25, 37.5, 50, 75, 100, 125, 150, 175, 200 μL of samples were taken and diluted with bidistilled water to 25 ml. Same procedures were applied to prepare phosphate buffer solutions with pH 3 and pH 7.4, respectively.

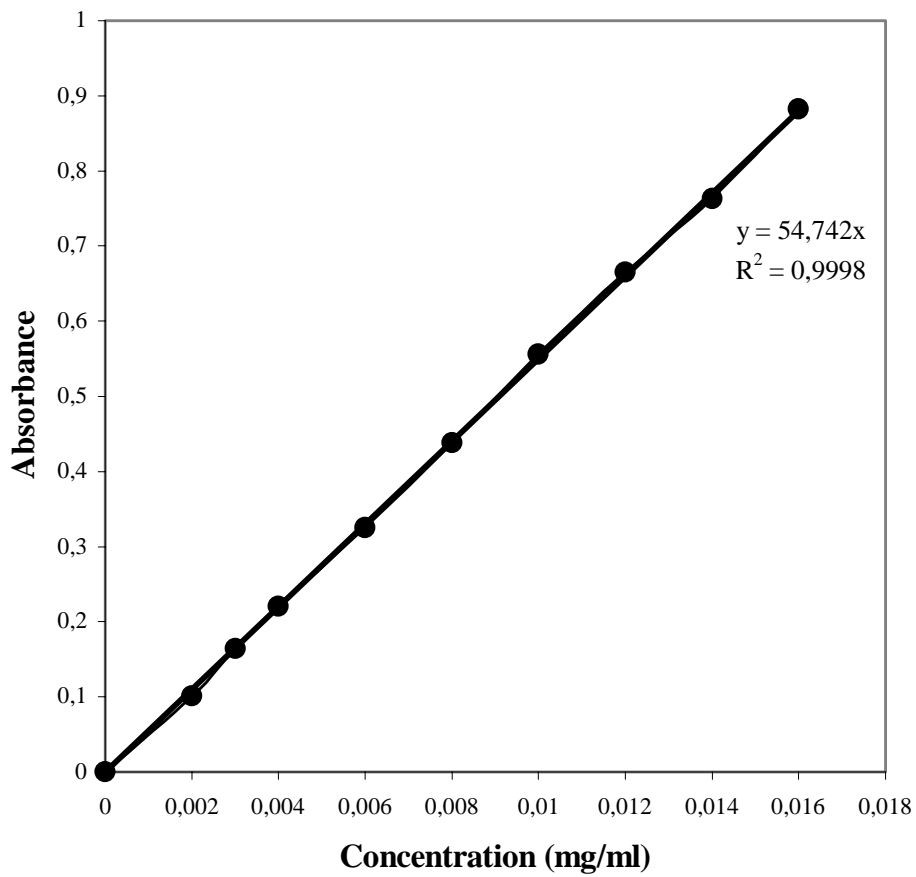


Figure B.1. Calibration curve of theophylline in water solution.

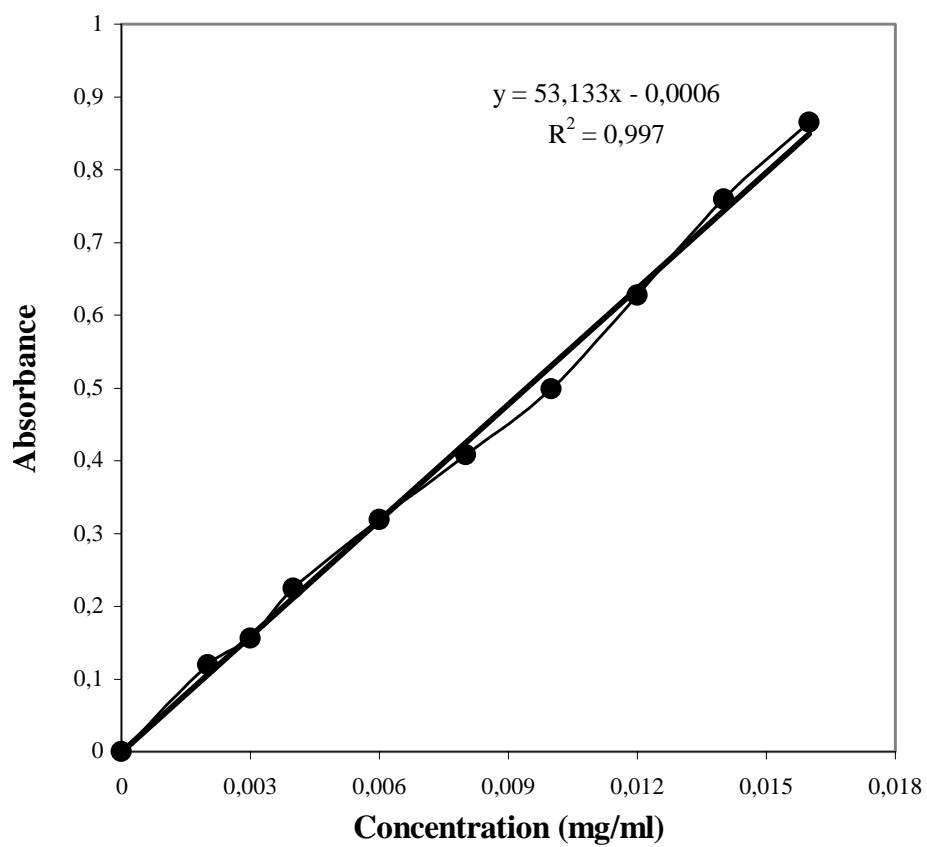


Figure B.2. Calibration curve of theophylline in pH 3 phosphate buffer solution.

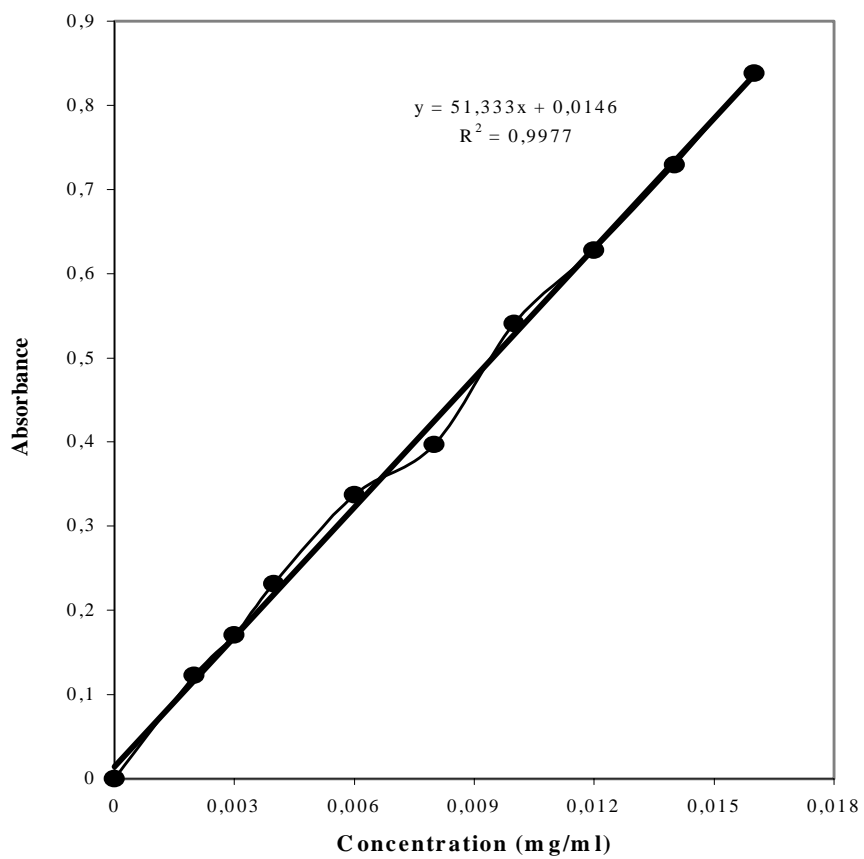


Figure B.3. Calibration curve of theophylline in pH 7.4 phosphate buffer solution.

APPENDIX C

Output of DESIGN-EXPERT

Response: release rate

ANOVA for Mixture Special Cubic Model

Analysis of variance table [Partial sum of squares]

<i>Source</i>	<i>Sum of Squares</i>	<i>DF</i>	<i>Mean Square</i>	<i>F Value</i>	<i>Prob > F</i>	
<i>Model</i>	0.17	6	0.028	39.97	< 0.0001	<i>significant</i>
<i>Linear Mixture</i>	0.14	2	0.069	98.25	< 0.0001	
<i>AB</i>	0.014	1	0.014	20.29	0.0028	
<i>AC</i>	7.212E-003	1	7.212E-003	10.30	0.0149	
<i>BC</i>	4.123E-003	1	4.123E-003	5.89	0.0457	
<i>ABC</i>	4.779E-003	1	4.779E-003	6.82	0.0348	
<i>Residual</i>	4.902E-003	7	7.003E-004			
<i>Lack of Fit</i>	8.518E-004	3	2.839E-004	0.28	0.8378	<i>not significant</i>
<i>Pure Error</i>	4.050E-003	4	1.013E-003			
<i>Cor Total</i>	0.17	13				

The Model F-value of 39.97 implies the model is significant. There is only a 0.01% chance that a "Model F-Value" this large could occur due to noise.

Values of "Prob > F" less than 0.0500 indicate model terms are significant.

In this case Linear Mixture Components, AB, AC, BC, ABC are significant model terms.

Values greater than 0.1000 indicate the model terms are not significant.

If there are many insignificant model terms (not counting those required to support hierarchy), model reduction may improve your model.

The "Lack of Fit F-value" of 0.28 implies the Lack of Fit is not significant relative to the pure error. There is a 83.78% chance that a "Lack of Fit F-value" this large could occur due

to noise. Non-significant lack of fit is good -- we want the model to fit.

Std. Dev.	0.026	R-Squared	0.9716
Mean	0.099	Adj R-Squared	0.9473
C.V.	26.82	Pred R-Squared	0.8851
PRESS	0.020	Adeq Precision	16.631

The "Pred R-Squared" of 0.8851 is in reasonable agreement with the "Adj R-Squared" of 0.9473.

"Adeq Precision" measures the signal to noise ratio. A ratio greater than 4 is desirable. Your ratio of 16.631 indicates an adequate signal. This model can be used to navigate the design space.

Component	Coefficient		Standard Error	95% CI	
	Estimate	DF		Low	High
A-CA	0.52	1	0.19	0.076	0.96
B-Ac	0.31	1	0.019	0.27	0.36
C-W	0.48	1	0.18	0.047	0.92
AB	-1.66	1	0.37	-2.52	-0.79
AC	-1.98	1	0.62	-3.44	-0.52
BC	-0.88	1	0.36	-1.74	-0.022
ABC	2.41	1	0.92	0.23	4.60

Final Equation in Terms of Pseudo Components:

$$\begin{aligned}
 \text{release rate} &= \\
 &+0.52 \quad * A \\
 &+0.31 \quad * B \\
 &+0.48 \quad * C \\
 &-1.66 \quad * A * B \\
 &-1.98 \quad * A * C \\
 &-0.88 \quad * B * C \\
 &+2.41 \quad * A * B * C
 \end{aligned}$$

Final Equation in Terms of Real Components:

$$\begin{aligned} \text{release rate} &= \\ &+40.38107 * CA \\ &+1.27250 * Ac \\ &+26.64414 * W \\ &-56.47210 * CA * Ac \\ &-260.60344 * CA * W \\ &-37.10052 * Ac * W \\ &+301.55970 * CA * Ac * W \end{aligned}$$

Final Equation in Terms of Actual Components:

$$\begin{aligned} \text{release rate} &= \\ &+40.38107 * CA \\ &+1.27250 * Ac \\ &+26.64414 * W \\ &-56.47210 * CA * Ac \\ &-260.60344 * CA * W \\ &-37.10052 * Ac * W \\ &+301.55970 * CA * Ac * W \end{aligned}$$

Diagnostics Case Statistics

Standard Order	Actual Value	Predicted Value	Residual	Leverage	Student Residual	Cook's Distance	Outlier t
1	0.18	0.19	-0.010	0.674	-0.669	0.132	-0.640
2	0.18	0.18	2.437E-003	0.438	0.123	0.002	0.114
3	0.054	0.063	-9.384E-003	0.647	-0.597	0.093	-0.567
4	7.200E-003	5.396E-003	1.804E-003	0.492	0.096	0.001	0.089
5	3.600E-003	1.529E-003	2.071E-003	0.442	0.105	0.001	0.097
6	0.36	0.31	0.047	0.492	2.506	0.869	7.226 *
7	3.600E-003	1.529E-003	2.071E-003	0.442	0.105	0.001	0.097
8	9.000E-003	0.015	-5.950E-003	0.326	-0.274	0.005	-0.255
9	0.18	0.18	2.437E-003	0.438	0.123	0.002	0.114
10	8.100E-003	5.396E-003	2.704E-003	0.492	0.143	0.003	0.133
11	0.27	0.31	-0.043	0.492	-2.267	0.711	-4.068 *
12	0.045	0.054	-8.652E-003	0.682	-0.580	0.103	-0.550
13	0.018	0.024	-5.796E-003	0.534	-0.321	0.017	-0.299
14	0.063	0.041	0.022	0.408	1.073	0.114	1.087

* Case(s) with |Outlier T| > 3.50

Proceed to Diagnostic Plots (the next icon in progression). Be sure to look at the:

- 1) Normal probability plot of the studentized residuals to check for normality of residuals.
- 2) Studentized residuals versus predicted values to check for constant error.
- 3) Outlier t versus run order to look for outliers, i.e., influential values.
- 4) Box-Cox plot for power transformations.